ELSEVIER

Marine Geology 225 (2006) 279–309

MARINE GEOLOGY
INTERNATIONAL JOURNAL OF MARINE GEOLOGY, GEOCHEMISTRY AND GEOPHYSICS

www.elsevier.com/locate/margeo

A record of fluctuating bottom currents on the slopes west of the Porcupine Bank, offshore Ireland — implications for Late Quaternary climate forcing

Lena K. Øvrebø *, Peter D.W. Haughton, Patrick M. Shannon

Department of Geology, University College Dublin, Belfield, Dublin 4, Ireland

Received 24 May 2004; received in revised form 17 June 2005; accepted 28 June 2005

Abstract

Both local and regional controls on slope sedimentation west of Porcupine Bank are assessed using an array of 25 gravity cores, integrated with shallow seismic, TOBI side-scan and high-resolution bathymetry data. The cores were retrieved from an area of smooth, distally steepened slope (between 52° and 53°N) in water depths of 950 to 2750 m. The slope here is unmodified by gravity failures and is swept by bottom currents that flow from S to N along the margin. The cores reveal a coherent shallow stratigraphy that can be traced along and between transects at upper-, mid- and lower-slope levels. AMS ^{14}C dating, oxygen-isotopes and carbonate profiles suggest the cored record could extend as far back as 500 ka in the longest cores, with most cores providing details of the slope response to the last interglacial, last glacial and Holocene forcing. The facies indicate deposition was dominated by a combination of bottom currents, ice-rafting and hemipelagic settling, with carbonate-prone deposits during interglacials, and siliciclastic deposits during glacials. Inferred contourites imply that strong currents operated during interglacials, with weaker current reworking during glacial conditions. A pair of erosion surfaces record significant mid- and upper-slope scouring during Marine Isotope Stage (MIS 3) and in the Early Holocene. The lateral facies distribution implies stronger currents at shallower levels on the slope, although there is evidence that the core of the current migrated up and down the slope, and that sand might locally have spilt down-slope. The bathymetry influenced both the wider geometry of the condensed contourite sheet and the local thickness and facies variation across the slope. A significant result of the study is the identification of a pair of thin sand–mud contourite couplets that record enhanced bottom-current reworking corresponding to periods of interstadial warming during MIS 3. The couplets can be correlated to the terrestrial records onshore Ireland and imply that the NE Atlantic margin oceanographic and onshore climate records are strongly coupled at interstadial level.

Keywords: Porcupine Bank; contourites; slope sedimentation; bottom currents; glacial cycles

* Corresponding author. Current address: Badley Ashton & Associates Ltd, Winceby House, Winceby, Horncastle, Lincolnshire, LN9 6PB, UK.

E-mail address: lovrebo@badley-ashton.co.uk (L.K. Øvrebø).

0025-3227/$ - see front matter © 2005 Elsevier B.V. All rights reserved.
doi:10.1016/j.margeo.2005.06.034

1. Introduction

Much work on contourites has been undertaken in areas of high sediment supply where large sediment drifts and extensive wave fields are developed (e.g. Cremer et al., 1993; Dowling and McCave, 1993; Masson et al., 2002; Stow and Holbrook, 1984; Stow et al., 2002; Wold, 1994). However, bottom currents are also important in areas of low sediment input. This paper assesses the history of bottom-current activity on the sediment-starved slopes to the west of the Porcupine Bank, on the Atlantic margin west of Ireland, against a backdrop of high-frequency Late Quaternary climate fluctuations. The slopes are close to the mouth of the trough and are exposed to a modern deep-water bottom-current system that sweeps the slopes from south to north. Significantly, the western flank of the Porcupine Bank has a large stretch of smooth and gentle upper slope (500 to 1200 m water depth) that is undisturbed by slope failures. This enables preservation of the background slope sedimentary succession without the complication of gravity remobilisation. The Porcupine Bank slope has also been extensively cored allowing a detailed reconstruction of the Late Quaternary shallow slope stratigraphy at different levels on the slope.

Both local and regional factors will potentially control sedimentation on an undersupplied ocean-facing slope system. Regional controls include changing sediment supply (both flux and type), variable current velocities and, during glaciation, episodes of ice-rafting. However, the presence of local factors such as slope failures and topographic irregularities can complicate the depositional signal produced by regional factors. To date, most studies addressing regional controls such as climate or ice-rafting flux are based on a single vertical core (e.g. Elliot et al., 2002; Knutz et al., 2001; Labeyrie et al., 1999; Lagerklint and Wright, 1999; Shackleton et al., 1984; van Kreveld et al., 1996). This, however, might not provide a complete picture, particularly in slope settings, as erosive and non-depositional hiatuses are often identified only through lateral correlations across an array of boreholes. The present study aims to identify and distinguish between local and regional controls on sedimentation using a large number of correlated cores on the Porcupine Bank slope. The spacing of the cores varies from grids of cores spaced 1 km apart to isolated cores spaced tens of kilometres apart. This allows both short- and long-scale correlations to be built and validated, and the wider 3D structure of the slope deposits to be reconstructed.

2. Regional setting

The Rockall Trough (Fig. 1), offshore western Ireland, is an elongate bathymetric depression trending approximately NNE–SSW. It is 1000 km long and 250 km wide with narrow marginal slopes (10–40 km wide) with gradients ranging from 2° to >20°. The trough extends from the Porcupine Abyssal Plain in the southwest (c. 52°N) to the Wyville–Thomson Ridge in the northeast (60°N). It is flanked to the west by the Rockall Bank and to the southeast by the Porcupine Bank. The water depths along the axes of the trough increase southwards from 1200 m in the north to 4500 m in the south.

The bathymetric configuration of the Rockall Trough has changed little since the mid-Cenozoic when late Eocene–Oligocene differential subsidence deepened the trough, forming the marginal slopes (Stoker et al., 2005). This deepening was associated with the onset of bottom-current circulation in the region (Stoker, 1997; Stoker et al., 2001). By the early Miocene, the Greenland–Scotland Ridge (including the Wyville–Thomson Ridge) was submerged and deep-water exchange between the Arctic and North Atlantic oceans was established (Boldreel and Andersen, 1995; Tucholke and Mountain, 1986) allowing northerly-derived water masses (*Norwegian Sea Deep Water*; NSDW) to enter the Rockall Trough. Davies et al. (2001) suggested an early Oligocene initiation of *North Atlantic Deep Water* (NADW) formation, which is the result of mixing of NSDW with surrounding water masses. The early Miocene to the early Pliocene was thus characterised by strong deep-water bottom-current circulation resulting in the accumulation and development of contourite sediment drifts and waves in the region (Stoker et al., 2001). The Plio-Pleistocene transition was marked by a period of major cooling in the North Atlantic and the initiation of Northern Hemisphere glaciation. Early Pliocene to Holocene sedimentation was influenced by climatic changes and sea-level fluctuations, and was characterised by further drift accumulation.

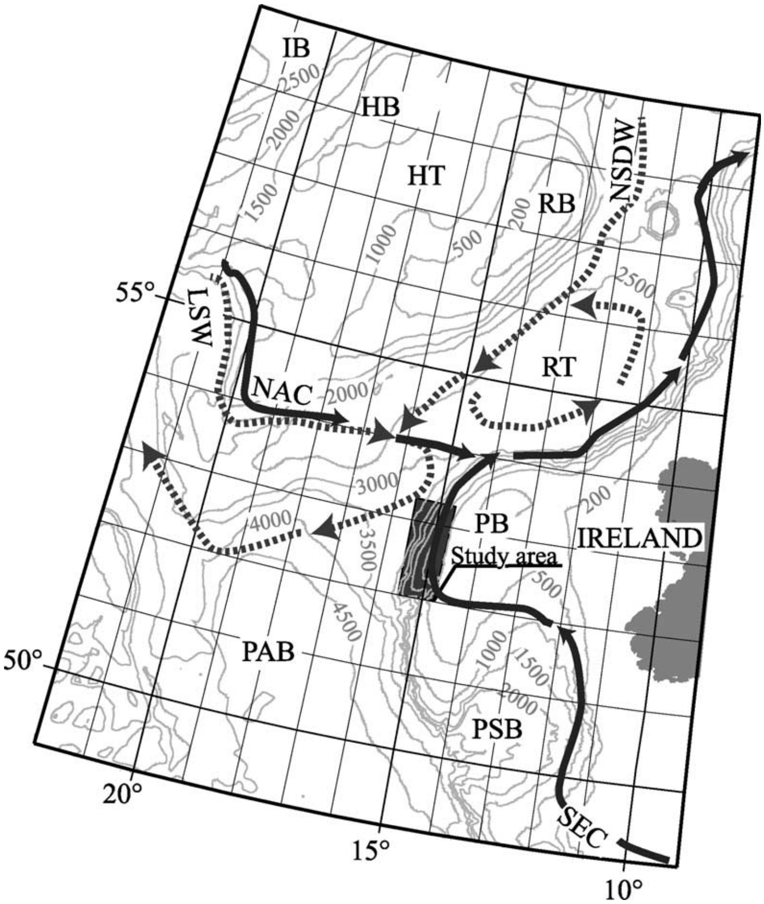

Fig. 1. Map of the Rockall Trough showing the modern ocean current circulation (see text for further discussion) and the location of the study area. Abbreviations: PAB = Porcupine Abyssal Plain; PSB = Porcupine Seabight; RT = Rockall Trough; PB = Porcupine Bank; HS = Hebrides Shelf; RB = Rockall Bank; HT = Hatton Trough; HB = Hatton Bank; IB = Iceland Basin; NAC = North Atlantic Current; SEC = Slope Edge Current; NSDW = Norwegian Sea Deep Water; and LSW = Labrador Sea Water.

The study has focused on the Late Quaternary, which was characterised by large changes in environmental conditions manifested by a succession of glacial and interglacial episodes. During the glacials, the climatic conditions varied from stadial periods with extensive glaciation of the Irish mainland to warmer periods termed interstadials or cold phases when near ice-free conditions prevailed in Ireland. The terrestrial record of glacials and interglacials can be correlated to the marine record, where the Holocene corresponds to Marine Isotope Stage (MIS) 1, the last glacial (Midlandian) to MIS 2–5d and the previous interglacial to MIS 5e (see Coxon, 2001).

The extent of the Quaternary glaciations off the west coast of Ireland and the UK is uncertain and poorly constrained. The onshore glacial record shows that Ireland was covered by ice sheets at least twice during the last glacial (the Midlandian, MIS 2–5d; see Coxon, 2001). The evidence for the extent of the glaciation is sparse on the Irish Shelf and parts of Ireland are often assumed to have been ice-free during the Midlandian glacial (Bowen et al., 1986). Warren (1992) reassessed the onshore glacial sedimentary record and morphology of Ireland, and his work indicates that almost all of Ireland was ice-covered and that the ice might have extended offshore. An offshore extension of the ice sheet could explain the abundant pebbles and boulders of possible Irish provenance extending from the bank crest and down the slope of the north Porcupine

Bank (Scoffin and Bowes, 1988). Recently, iceberg ploughmarks have also been recognised on the north Porcupine Bank, on the seabed above the Connemara oil accumulation and in the shallow subsurface (Games, 2001). Ploughmarks have also been recognised near the margins of the Porcupine Bank on Geological Survey of Ireland (GSI) multibeam bathymetry data, but details have not yet been published (Xavier Monteys, GSI, personal communication).

The present-day oceanographic circulation in the Rockall Trough (Fig. 1) is complex (see e.g. Holliday et al., 2000; New and Smythe-Wright, 2001; New et al., 2001; Read, 2001), and only the key water masses and currents affecting the study area on the Porcupine Bank will be discussed here (see Fig. 1). A saline *East North Atlantic Water* (ENAW) mass formed in the Bay of Biscay and, carried by a poleward S*helf-Edge Current* (SEC) along the European continental shelf, enters the Rockall Trough from the south (Ellett et al., 1986; Huthnance, 1986; Pollard et al., 1996). Fresher water masses, termed *Sub-Arctic Intermediate Water* (SAIW), enter the Rockall Trough from the west and are carried by a branch of the *North Atlantic Current* (NAC; McCartney and Mauritzen, 2001). This current moves eastwards from the western North Atlantic before it turns northwards and through the Rockall Trough mixing with the more saline ENAW (Ellett et al., 1986). The deeper waters in the trough have characteristics that are associated with *Labrador Sea Water* (LSW). This water mass originates in the Labrador Sea (Talley and McCartney, 1982) and enters the Rockall Trough from the southwest. The simulations of New and Smythe-Wright (2001) suggest that LSW circulates cyclonically in the basin, fed from the southwest by a strong inflow along 54°N and from the north by overflows from the Wyville–Thomson Ridge (NSDW) along 12°W. NSDW sinks rapidly as it moves southwards the western margin of the trough. There is much mixing and entrainment of surrounding water as it propagates southwards and the net result is the formation of a salinity maximum at 2300–2500 m depth termed *North-East Atlantic Deep Water* (NEADW; Ellett and Martin, 1973; van Aken and Becker, 1996).

The present paper concentrates on the western slopes of the Porcupine Bank, along the southeast margin of the Rockall Trough (Fig. 2). The slopes flanking the Porcupine Bank typically have gradients of 3°–4°. The shelf break is located at c. 600 m water depth and base-of-slope at c. 3000 m water depth (Fig. 2). The studied slope (52° to 53°20′N)

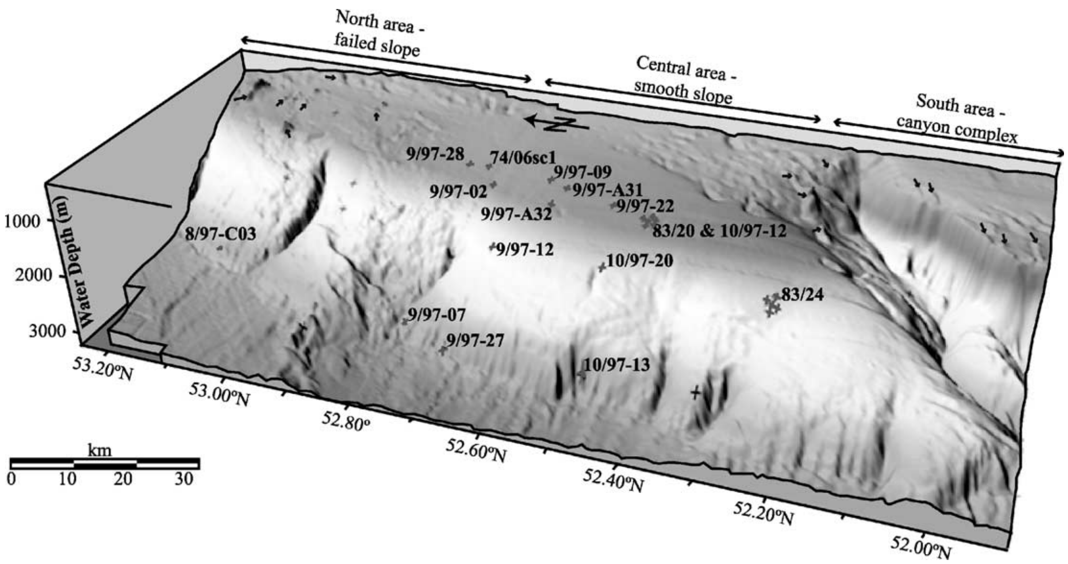

Fig. 2. 3D Bathymetry map of the Porcupine Bank showing the location of the gravity cores available on the margin of the bank. The black arrows identify carbonate mounds. (Bathymetry data courtesy of Geological Survey of Ireland.)

can be divided into three areas on the basis of the slope morphology, as revealed by TOBI imagery and high-resolution bathymetry data. In the southern area (51°35′ to 52°15′N) a NE–SW oriented canyon complex is present (Unnithan et al., 2001). The canyon originates at the bank margin, and the gradients along the canyon walls exceed 20°. The present sediment input into the canyon system is low and the area is starved of sediment. This might provide suitable conditions for the development of deep-water carbonate mounds, which are present up-slope of the canyon head. The shallower slopes between 52°15′N and 52°45′N are smooth with low backscatter on TOBI images (Fig. 3). The upper slope is characterised by low gradients (1°–3°), whilst the deeper slopes steepen distally to 9° and locally up to 20°. The bathymetry data (Fig. 2) reveal that the steeper lower part of the slope is heavily incised by a series of canyons (up to 250 m deep and 2–5 km wide) and gullies (50 m deep and up to 1 km wide) that originate at a mid-slope inflection at c. 2000 m. Shallow seismic from the area shows a smooth seabed and an up-slope thickening of the top Plio-Pleistocene unit (Fig. 4) that Haughton et al. (2005) attributed to widespread bottom-current activity.

North of 52°45′ and extending to 53°20′N, the slope morphology is more complex and uneven, with a combination of canyons, slope failure escarpments, slump deposits and current lineations imaged by side-scan sonar and bathymetry surveys (Fig. 3). In the upper-slope region (500 to 1000 m water depth)

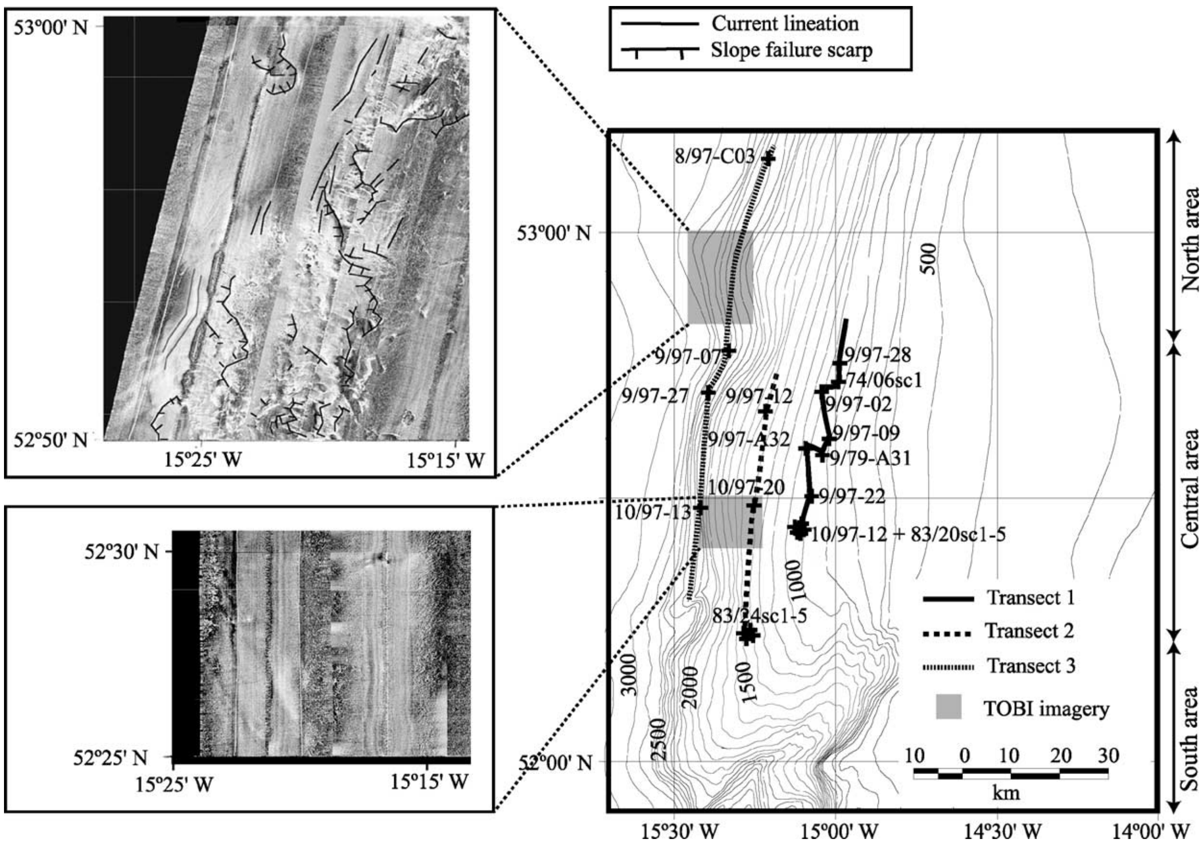

Fig. 3. Map showing the studied gravity cores distributed along three transects on the western slopes of the Porcupine Bank together with examples of TOBI side-scan imagery of the seabed. The TOBI imagery shows that the central area has a smooth seabed with low backscatter, while in the northern area the backscatter is high with current lineations and slope failure scarps. Interpretations of TOBI imagery are from O'Reilly et al. (2001).

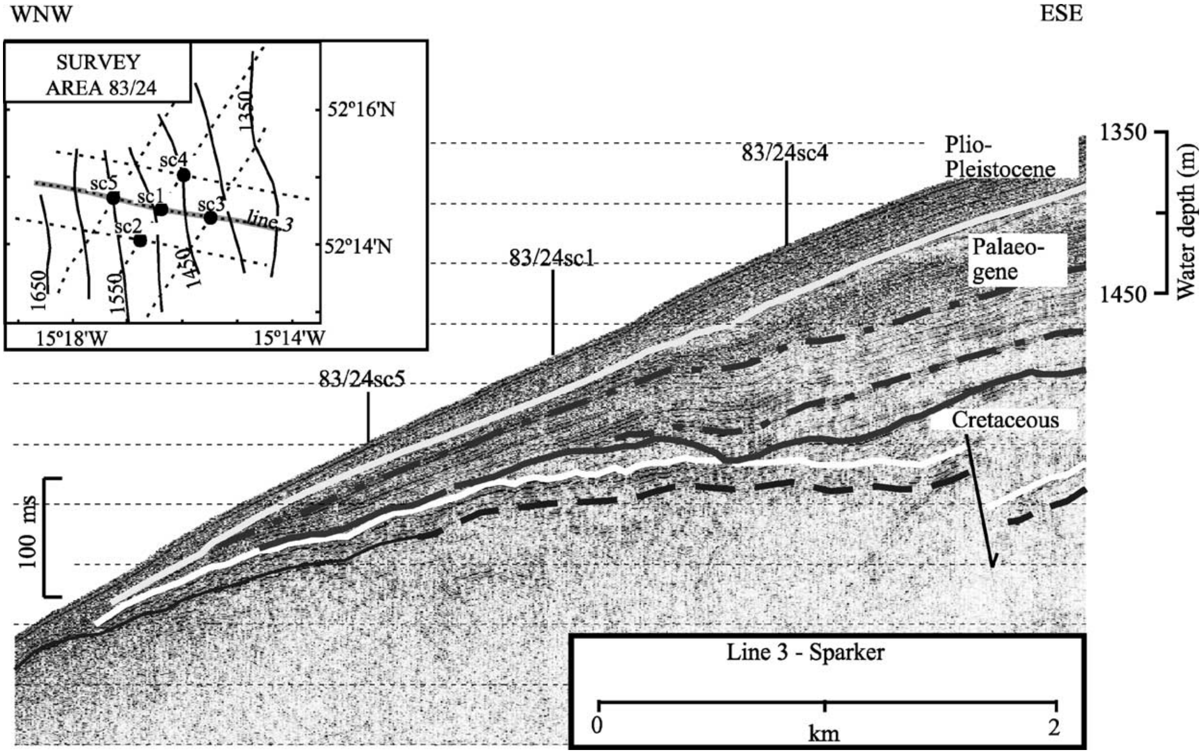

Fig. 4. Shallow seismic line showing an up-slope thickening of the Plio-Pleistocene unit interpreted as a contourite. Modified from Haughton et al. (2005).

seabed imaging reveals a field of carbonate mounds (Fig. 2) referred to as the Pelagia Mound Province (e.g. Kenyon et al., 2003; O'Reilly et al., 2003).

3. Materials and methods

An extensive programme of shallow gravity coring was undertaken by the *M.V. Challenger* during 1998 on the slopes flanking the Rockall Trough. The cores were taken in preparation for deeper stratigraphic drilling in the area on behalf of the Rockall Studies Group (RSG). A further suite of gravity cores was collected during the summer of 1999 by the *M.V. Polarboy*. A subset of 24 of the cores from both these cruises, located on the smooth slopes on the western flanks of the Porcupine Bank, were logged and studied. The cores range from <1 m to 2.70 m in length and they include two clusters of five and six cores spaced 1 km apart on grids tied by high-resolution seismic profiles surrounding the RSG deeper stratigraphic borehole sites in Irish offshore blocks 83/20 and 83/24. In addition, a series of cores, spaced 4 to 30 km apart and distributed along three transects across the upper, mid and lower parts of the slope (transects 1 to 3, respectively), were studied in order to constrain the lateral distribution and character of the deposits draping the slopes (Fig. 3; Table 1).

Prior to sedimentological logging, x-radiographs were taken of three cores. This was done in order to reveal any cryptic structures in the cores (e.g. subtle laminations, bioturbation, and dropstones). Subsequently stable oxygen-isotope profiles, carbonate-content measurements, grain-size analyses, grain counting and ^{14}C AMS dating have been undertaken. The stable isotope work was performed on samples spaced 5 cm apart in core 83/24sc5. The samples were dispersed in 0.1 M Calgon solution over night. These samples were then wet-sieved and 20–30 specimens of *Globigerina bulloides* were handpicked from the >250-μm fraction.

Table 1
Summary of the gravity cores studied on the slopes west of Porcupine Bank, offshore Ireland

Core no.	Length (m)	Water depth (m)	Latitude/Longitude	Position on slope
83/20-sc1	1.68	1060	52°26.77′N, 15°07.72′W	Transect 1
83/20-sc2	1.94	1025	52°27.12′N, 15°25.22′W	Transect 1
83/20-sc3	2.29	1032	52°26.65′N, 15°06.86′W	Transect 1
83/20-sc4	1.99	1043	52°26.15′N, 15°07.26′W	Transect 1
83/20-sc5	2.06	1007	52°26.45′N, 15°05.98′W	Transect 1
10/97-12	2.44	1030	52°26.01′N, 15°06.60′W	Transect 1
09/97-22	1.83	1000	52°30.25′N, 15°04.58′W	Transect 1
09/97-A31	1.18	955	52°34.91′N, 15°02.53′W	Transect 1
09/97-A32	1.77	1090	52°35.67′N, 15°05.67′W	Transect 1
09/97-09	0.90	924	52°36.75′N, 15°01.34′W	Transect 1
09/97-02	1.39	1081	52°42.04′N, 15°02.73′W	Transect 1
74/06-sc1	1.98	978	52°43.18′N, 14°59.59′W	Transect 1
09/97-28	1.42	1003	52°45.27′N, 14°59.33′W	Transect 1
83/24-sc1	1.51	1468	52°14.55′N, 15°16.35′W	Transect 2
83/24-sc2	2.54	1503	52°14.06′N, 15°16.26′W	Transect 2
83/24-sc3	1.93	1404	52°14.43′N, 15°15.47′W	Transect 2
83/24-sc4	1.34	1426	52°15.07′N, 15°16.00′W	Transect 2
83/24-sc5	2.54	1527	52°14.68′N, 15°17.26′W	Transect 2
10/97-20	3.14	1432	52°29.18′N, 15°15.26′W	Transect 2
09/97-12	2.38	1572	52°39.83′N, 15°13.13′W	Transect 2
10/97-13	2.50	2562	52°28.95′N, 15°25.22′W	Transect 3
09/97-27	2.56	2756	52°41.95′N, 15°23.77′W	Transect 3
09/97-07	2.92	2719	52°46.71′N, 15°19.93′W	Transect 3
08/97-C03	2.61	2535	53°08.22′N, 15°12.64′W	Transect 3

The samples were sent to the Godwin Laboratory at the University of Cambridge for stable isotope measurements. The foraminifera were crushed and cleaned by soaking in 3% hydrogen peroxide and subjected to ultrasound for a few seconds. The oxygen-isotope measurements were performed on a VG SIRA mass spectrometer. The precision of the analyses is <0.08 ‰.

High-resolution (measurements every 5 to 10 cm) carbonate profiles were also generated for key cores on the slope. A small sample (0.1–0.2 mg) was dried, crushed, weighed and dissolved in HCl. The carbonate content was then measured using a Scheibler Calcimeter (Müller, 1967). The results can be reproduced with an accuracy of less than 5%.

Grain size was determined at the Department of Geography in University College Cork using a Malvern Mastersizer 2000, which measures grain sizes ranging from 0.02 to 2000 μm. Selected samples from the most common lithofacies were dispersed in Calgon solution prior to laser grain-size analyses. Grain counting was undertaken on the >150 μm fraction of samples spaced 5–10 cm apart in the cores. The samples were dried and sieved and then split down to fractions of approximately 200–300 grains using a microsplitter. The counting procedure distinguished five grain categories: Ice-rafted debris (IRD; mineral grains and rock fragments >150 μm); total foraminifera; *N. pachyderma* sinistral; *N. pachyderma* dextral and *G. bulloides*. The total contents of lithics and foraminifera are presented in number of grains per gram sediment, whereas the individual foraminifera species are presented in percent of the total foraminifera content.

Eleven samples for dating were dispersed in Calgon solution, sieved and 10 mg of various planktonic foraminifera were handpicked from the >250-μm fraction. The planktonic foraminifera were sent to SUERC Radiocarbon Dating Laboratory for AMS ^{14}C dating. The radiocarbon ages up to 24 000 years were calibrated to calendar ages using CALIB 4.3 (Stuiver and Reimer, 1993; Stuiver et al., 1998). Radiocarbon ages older than 24 000 years were calibrated using Th–U ages obtained by mass spectrometry on corals (Bard, 1998) after subtracting 400 ^{14}C years for reservoir correction.

4. Core sedimentology

The gravity cores retrieved from the smooth section of the Porcupine Bank slope reveal a detailed stratigraphic succession with units 1–30 cm thick that can be followed from core to core along and between the transects. Four main lithofacies were identified based on lithology, texture, presence of coarsening/fining-upward sequences, the nature of contacts, and sedimentary structures (summarised in Tables 2 and 3):

1. *Lithofacies H-1:* Moderately-sorted muddy deposits.
2. *Lithofacies IH-1:* Poorly- to moderately-sorted muddy deposits with ice-rafted debris (IRD).
3. *Lithofacies P-1:* Carbonate-rich deposits.
4. *Lithofacies C-1 to 3:* Moderately- to well-sorted and occasionally bedded sands.

4.1. Lithofacies H-1 — moderately-sorted muddy deposits

Lithofacies H-1 is present in the majority of the cores along the upper-slope transect 1, but is absent deeper on the slope. H-1 is a structureless dark yellowish brown mud (Fig. 5) with both scattered and clustered in situ sponge spicules identified as *Demospongiae Spirophoridea Tedilidea* (Jean Vacelet, Centre d'Oceanographie de Marseille, personal communication). The overall foraminifera content is low, but dominated by *N. pachyderma* sinistral (see Table 3). Bioturbation intensity is low with a network of mm-sized, narrow vertical burrows. Grain-size analysis (Fig. 6) reveals a moderately-sorted mud, with a sand component (>63 μm) amounting to only 1.5%. The basal contact is gradational and Lithofacies H-1 passes gradationally into the underlying lithofacies IH-1.

4.1.1. Interpretation

Lithofacies H-1 is interpreted to represent hemipelagic settling based on the poor sorting and the

Table 2
A summary of the main lithofacies recognised in gravity cores from the Porcupine Bank slopes, offshore Ireland

Characteristics	Lithofacies H-1	Lithofacies IH-1	Lithofacies P-1	Lithofacies C-1	Lithofacies C-2 and 3
Colour (Munsell colour chart representations)	Dark yellowish brown (10YR 4/2).	IH-1a: moderate yellowish brown (10YR 5/4). IH-1b: light olive grey (5Y6/1).	Greyish orange to very pale orange (10YR7/4-8/2).	Pale yellowish brown (10YR 6/2).	Pale yellowish brown (10YR 6/2).
Lithology	Mud.	Sandy mud.	P-1a and b: sand. P-1c and d: clay.	C-1a: muddy sand. C-1b: sandy mud.	Sand.
Sedimentary structures	None.	Occasional grading.	Reverse+normal grading. P-1a and d: bioturbated.	Mottled.	C-2: normal grading. C-3: bedding+bioturbation.
Contacts	Gradational base.	Gradational to occasional sharp contacts.	Gradational to sharp.	Sharp, irregular base.	C-2: sharp to erosive base. Biturbated top. C-3: sharp contacts.
Carbonate content	20–21%.	6–34%.	45–70%.	45–53%.	30–51%.
IRD (lithics>150 μm, see Table 3)	Rare.	Abundant.	Rare.	Rare to common.	Common.
Microfossils (see Table 3)	Foraminifera+sponge spicules.	Foraminifera.	Foraminifera+coccoliths.	Mainly foraminifera.	Foraminifera.
Setting	Upper slope levels.	All slope levels.	All slope levels.	All slope levels.	C-2: upper+mid-slope. C-3: base of slope.
Depositional mechanism	Hemipelagic settling.	Ice-rafting+hemipelagic settling. IH-1a reworked by weak bottom currents.	Pelagic settling, bottom current reworked.	Bottom current reworking and deposition.	

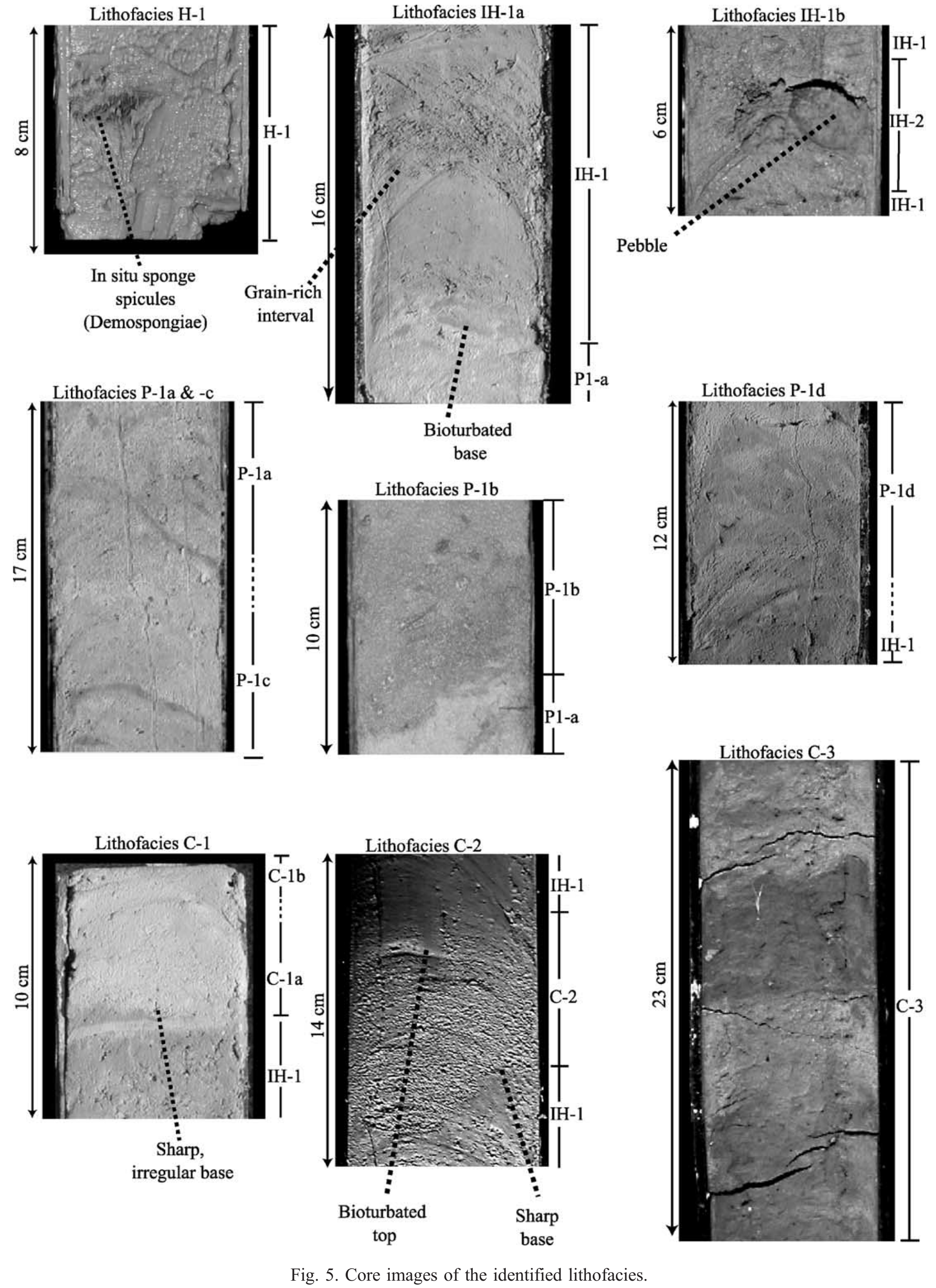

Fig. 5. Core images of the identified lithofacies.

Table 3
The results of counting of 64 samples of the main lithofacies identified on the Porcupine Bank slope

Lithofacies	No. of samples counted	Sand Component (>150 μm; 10^3 grains/g)			Foraminifera			Comments
		Total	Lithics	Foraminifera	*G. bulloides*	*N. pachyderma* dextral	*N. pachyderma* sinistral	
H-1	10	2–8	1–2	1–6	R	R	A	Sponge spicules (*Demospongiae Spirophoridea Tedilildea*) are common.
IH-1	29	5–58	2–15	1.5–41	B–C	T–F	A–D	Rare sponge spicules+bivalve fragments.
P-1a	2	125–150	1–1.5	124–148	F	C	R	
P-1b	2	38–134	2–2.5	35–125	F	F	F–C	
P-1c+d	7	18–60	0.2–1.7	18–60	F	C	F	
C-1a	2	9–13.5	0.5–1.5	7–13	F	C	R–F	
C-1b	3	11–15	2–15.6	3–9	R	C–D	B–F	The high lithic content is due to concentration of lithics near base of the facies.
C-2+3	7	20–110	2.5–10.5	15.6–106.5	C	C	R–F	

Abbreviations: B=Barren (absent); T=Trace (<1%); R=Rare (>15%); F=Few (>510%); C=Common (>1030%); A=Abundant (3060 %); D=Dominant (>60%). The sponge spicules in lithofacies H-1 were identified by Jean Vacelet (Centre d'Oceanographie de Marseille).

absence of primary sedimentary structures. The high cold-water foraminifera content and the presence of *Demospongiae* indicate that these sediments were deposited during a cold period. The sponges characteristically occur on soft substrates that they are able to colonise through the development of a basal mat of tangled spicules (Jean Vacelet, personal communication). The network of burrows in H-1 and the absence of large burrows indicate anaerobic waters. H-1 thus represents hemipelagic mud deposition in an area where bottom currents were very weak, thus allowing large quantities of mud to be deposited.

4.2. Lithofacies IH-1 — poorly- to moderately-sorted muddy deposits with IRD

Lithofacies IH-1 is the most common lithology encountered and is developed at several levels in all the cores. It can be divided into subfacies IH-1a and b, where IH-1a is most common. Both facies are sandy mud with scattered lithic clasts ranging in size from coarse sand to pebbles 2 cm across. The upper and basal contacts are sharp to gradational and bioturbated (Fig. 5). Subfacies IH-1a is moderate yellowish brown in colour. Bioturbation has obscured primary sedimentary structures, although x-radiographs show a weak primary lamination in places (Fig. 7). The sorting is poor to moderate but with a minor peak at 5 μm and it has a variable concentration of IRD (ice-rafted debris) giving rise to a sand content of 25% to 50% and occasional grading of the deposits. Subfacies IH-b comprises poorly-sorted (Fig. 6), structureless and olive grey 1 to 5 cm thick mud bands that rest on subfacies IH-1a.

4.2.1. Interpretation

The poor sorting and lack of sedimentary structures, the high clay content and high content of lithic grains suggest that the facies is a result of a combination of hemipelagic deposition, ice-rafting and bioturbation mixing. The variable IRD content of IH-1a can be explained by temporal variations in the ice-rafted sediment flux. Several authors have reported that ice-rafting varied with time in the North Atlantic, with peaks in IRD attributed to Heinrich Events (e.g. Abrantes et al., 1998; Bond et al., 1992; Bond and Lotti, 1995; Bowen et al., 2002; Heinrich, 1988). An alternative explanation for the variable IRD-content of IH-1a is the operation of bottom currents that varied in strength with time. These might preferentially suspend mud and thus cause higher concentrations of coarse lithic grains. The grain-size distribution (Fig. 6), with

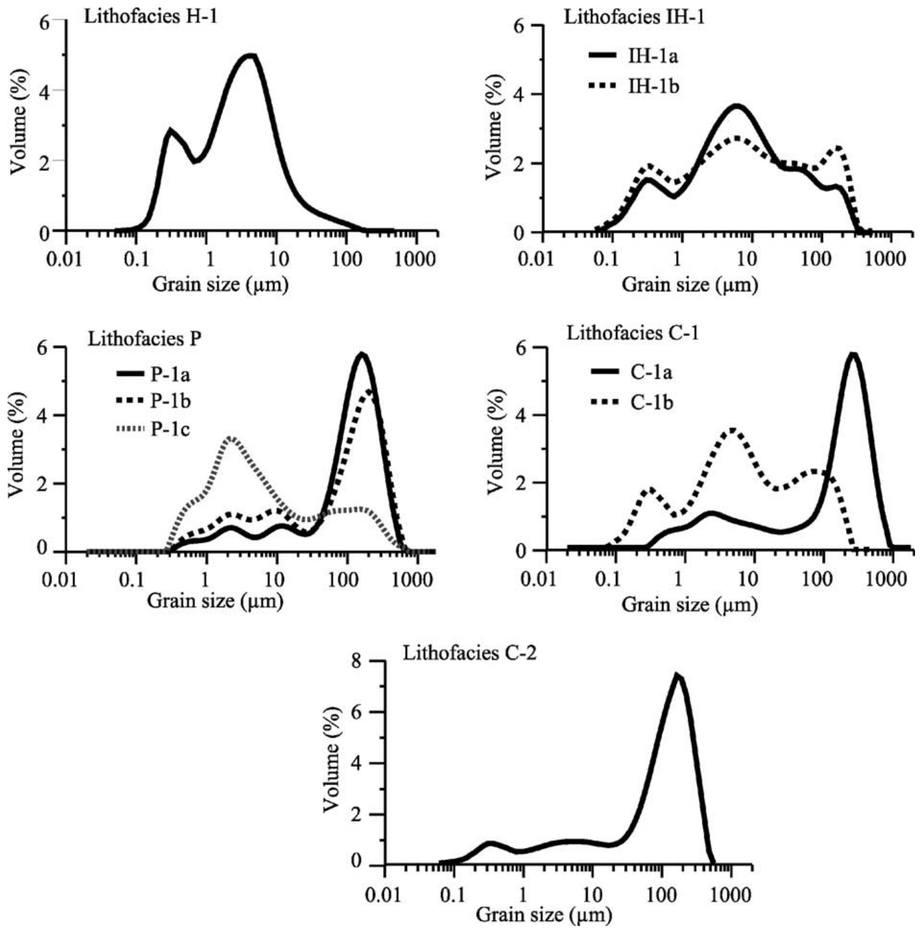

Fig. 6. Grain-size distribution of representative samples of facies H, IH, P and C. The diagrams are created from laser-grain sizing measurements.

a minor peak at 5 μm together with the occasional grading, suggests that weak bottom currents controlled the deposition of the mud. The moderate yellowish brown colour of the deposits is an indicator of well-ventilated bottom waters, which supports the presence of bottom currents. The grain-size distribution also indicates possible bottom-current activity. Most likely the bottom-current activity was superimposed upon a variable ice-rafting. Lithofacies IH-1a can thus be classified as a muddy contourite with ice-rafted debris. The thin and poorly-sorted lithofacies IH-1b, on the other hand, seems to be relatively unaffected by currents as evidenced by the poor sorting. IH-1b is therefore interpreted as an ice-rafted hemipelagite deposited in a period when bottom-current activity was very low.

4.3. Lithofacies P-1 — carbonate-rich deposits

Lithofacies P-1 comprises greyish orange to very pale orange, foraminiferal and nannofossil oozes (Fig. 5). Four subfacies (a to d) are identified on the basis of grain size and the degree of bioturbation. *Subfacies P-1a* is a bioturbated foraminiferal ooze that is moderately sorted with a pronounced mode in the sand fraction. The facies commonly passes gradationally downcore into the less bioturbated foraminiferal sand of *subfacies P-1b* with occasional sharp, internal contacts. The latter is moderately- to well-sorted and has a unimodal grain-size distribution with a mode at fine/medium sand grade (Fig. 6). P-1b sits gradationally on top of *subfacies P-1c*, which is a moderately-sorted nannofossil ooze. This subfacies is

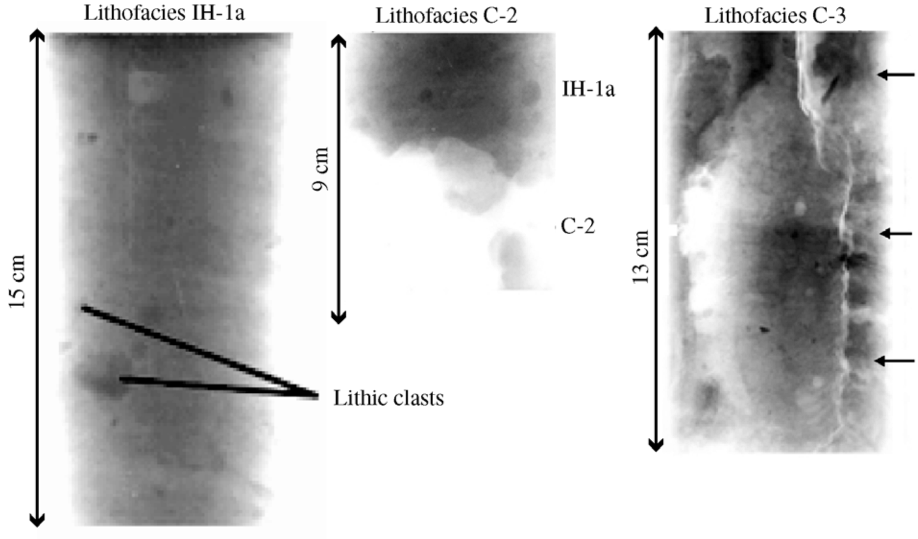

Fig. 7. X-radiographs of lithofacies IH and C. Lithofacies IH-1 have a weak and poorly preserved lamination. C-2 is structureless sand with a low degree of consolidation, thus letting most of the X-rays pass through it, giving rise to the bright colour on the x-radiograph. Notice the bedding (arrowed) picked out by the x-radiographs of lithofacies C-3.

separated by a transitional contact from the underlying *subfacies P-1d*. This is a bioturbated nannofossil ooze, which has a bioturbation fabric picked out by thin clay-filled horizontal and slightly inclined burrows. The entire facies association from P-1a to d is only preserved in cores at mid- and lower-slope levels, while at upper-slope levels only P-1a and b are preserved.

4.3.1. Interpretation

Lithofacies P-1 is interpreted as a pelagic ooze based on the high carbonate and bioclastic content. The deposits, however, display commonly reverse grading and a variable degree of bioturbation. A possible explanation for the reverse grading is a temporal change in the palaeoproduction from mainly coccoliths to foraminifera. However, this cannot account for the spatial and temporal variability in the bioturbation intensity, the occasional internal sharp contacts and the absence of the full facies succession (P-1a to d) in some of the cores. A more likely explanation is therefore that the pelagic deposits have been reworked by bottom currents, and that changes in the bottom-current velocity caused winnowing of the deposits, non-deposition and reduced settling of nannofossils. Lithofacies P-1 is therefore interpreted as a biogenic contourite, and this is supported by the grain-size data that indicate a degree of sorting. Current reworking could also account for the occasional internal sharp contacts, as these could be explained by local and temporal increases in current velocity. The locally gradational base of the biogenic contourites indicates a gradual increase in bottom-current velocity, while the sharp top is indicative of a sudden drop in the bottom-current velocity. Along the upper slope, only the coarser parts of the biogenic contourite (lithofacies P-1a and b) are preserved, suggesting that the currents here were strong enough to cause initial bypass or erosion. This would account for the absence of the fine-grained lithofacies P-1c and d at these levels of the slope. The absence of significant siliciclastic input or IRD suggests deposition during times of subdued glacial influx.

4.4. Lithofacies C — moderately- to well-sorted and occasionally bedded sands

Three subfacies, C-1 to 3, have been recognised within this sand-prone lithofacies. C-1 and C-2 are structureless deposits and are generally found at upper- and mid-slope levels (transects 1 and 2), whereas lithofacies C-3 is a laterally equivalent bedded sand that is developed on the lower slope (transect 3).

4.4.1. Subfacies C-1 — pale yellowish brown mottled mud and sands

Two variants are recognised, C-1a (moderately-sorted muddy sand) and C-1b (well-sorted sandy mud). Subfacies C-1a passes transitionally up into C-1b, where both are present (Fig. 5). It has a mixed terrigenous and biogenic composition (Table 3). The base of the facies is sharp and concentrations of lithic grains near the base are common. In places large (cm-scale) circular burrows pipe down sand from lithofacies C-1 into the underlying mud of lithofacies H-1 or IH-1.

4.4.2. Subfacies C-2 — pale yellowish brown moderately-sorted sand

This subfacies has a relatively low mud content as confirmed by the near unimodal grain-size distribution with a pronounced sand peak at 200 μm (Fig. 6). The base of subfacies C-2 is sharp to erosive, whereas the top contact is bioturbated. An enrichment of coarser grains can be observed along the base and this is especially evident where the base is erosive. The presence of basal erosion is established from the correlation of units across the grids of closely spaced cores, where it is evident that the underlying unit is locally partially or completely removed by erosion (see further discussion below). Primary structures are generally absent in both cores as confirmed by x-radiographs (Fig. 7). C-2 is most commonly associated with lithofacies IH-1.

4.4.3. Subfacies C-3 — bedded sand

This is a pale to dark yellowish brown sand with a gradational base. It is the only facies identified on the slope that has obvious internal bedding preserved (see Figs. 5 and 7). Two variants are recognised based on the degree of bioturbation. Subfacies C-3a has a low to moderate degree of bioturbation, while C-3b is thoroughly bioturbated and primary structures are partially or completely obscured. Locally, the only indication of a pre-existing sand bed is a dense array of sand-filled burrows. Both C-3a and C-3b are commonly associated with IH-1.

4.4.4. Interpretation

Lithofacies C has a combination of features that are characteristic of contourite deposition (e.g. Stow and Piper, 1984; Stow and Tabrez, 1998; Viana et al., 1998). These include the sharp to erosive base of lithofacies C-1 and 2, the moderate sorting, the unimodal grain-size distribution and the absence or poor preservation of primary structures. The microfossil assemblage (Table 3) and carbonate content might indicate that lithofacies C-1 is an interglacial deposit. The facies can thus be interpreted as interglacial sandy (C-1a) and muddy (C-1b) contourites where settling of mud and foraminifera have been controlled by the presence of bottom currents that can keep mud suspended or cause winnowing of pre-existing deposits. The mixed biogenic and terrigenous composition (Table 3) of lithofacies C-2 and 3, on the other hand, indicate that these are bottom-current reworked hemipelagic and ice-rafted deposits. The bedded nature of lithofacies C-3 suggests some variations in bottom-current strength during deposition.

5. Stratigraphy and lateral distribution of lithofacies

A vertical sequence of lithofacies is developed in each core and can be used to identify up to 17 lithostratigraphic units (numbered 1 to 17 downcore). These units can be correlated between the cores spaced 1 km apart in the 83/20 and 83/24 areas (Fig. 8) and over greater distances along and between the three transects (Figs. 9–11), although the unit thicknesses, contact styles and aspects of the facies do change both along and down slope. For description purposes the units have been grouped into three broad stratigraphic packages based on lithofacies associations (Table 4). The lowermost package, package III, comprises units 8 to 17 and is an alternation between biogenic contourites (lithofacies P-1; units 8, 10, 12, 14 and 16) and ice-rafted muddy contourites (lithofacies IH-1; units 9, 11, 13, 15 and 17). Package II (units 2 to 7) sits sharply on top of package III, and the first unit that was deposited was an ice-rafted muddy contourite (unit 7). This unit has been partially or completely removed at lower- and mid-slope levels by subsequent bottom-current erosion leading to the formation of a prominent erosion surface at this level. The surface forms the base of unit 6 which is a couplet comprising a sandy (unit 6a) and a muddy contourite (unit 6b), capped by a 1- to 2-cm-thick ice-rafted hemi-

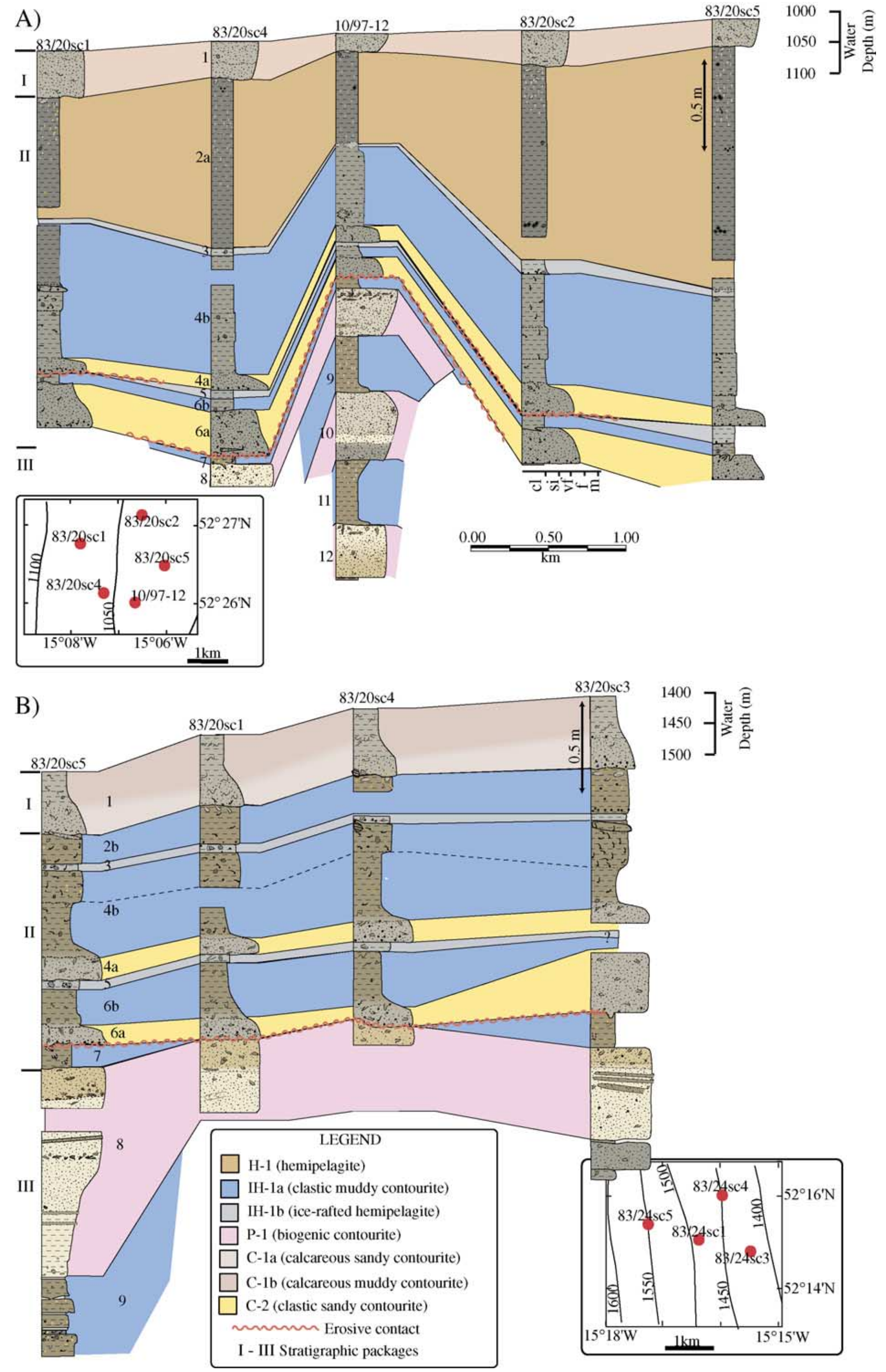

Fig. 8. Detailed correlation at km-scale between clusters of cores in the 83/20 area on the upper slope transect 1 (A) and in the 83/24 area on mid-slope transect 2 (B). Stratigraphic units are numbered 1 to 9 and stratigraphic packages I to III downcore. For regional-scale correlations across the slope see Figs. 9–11.

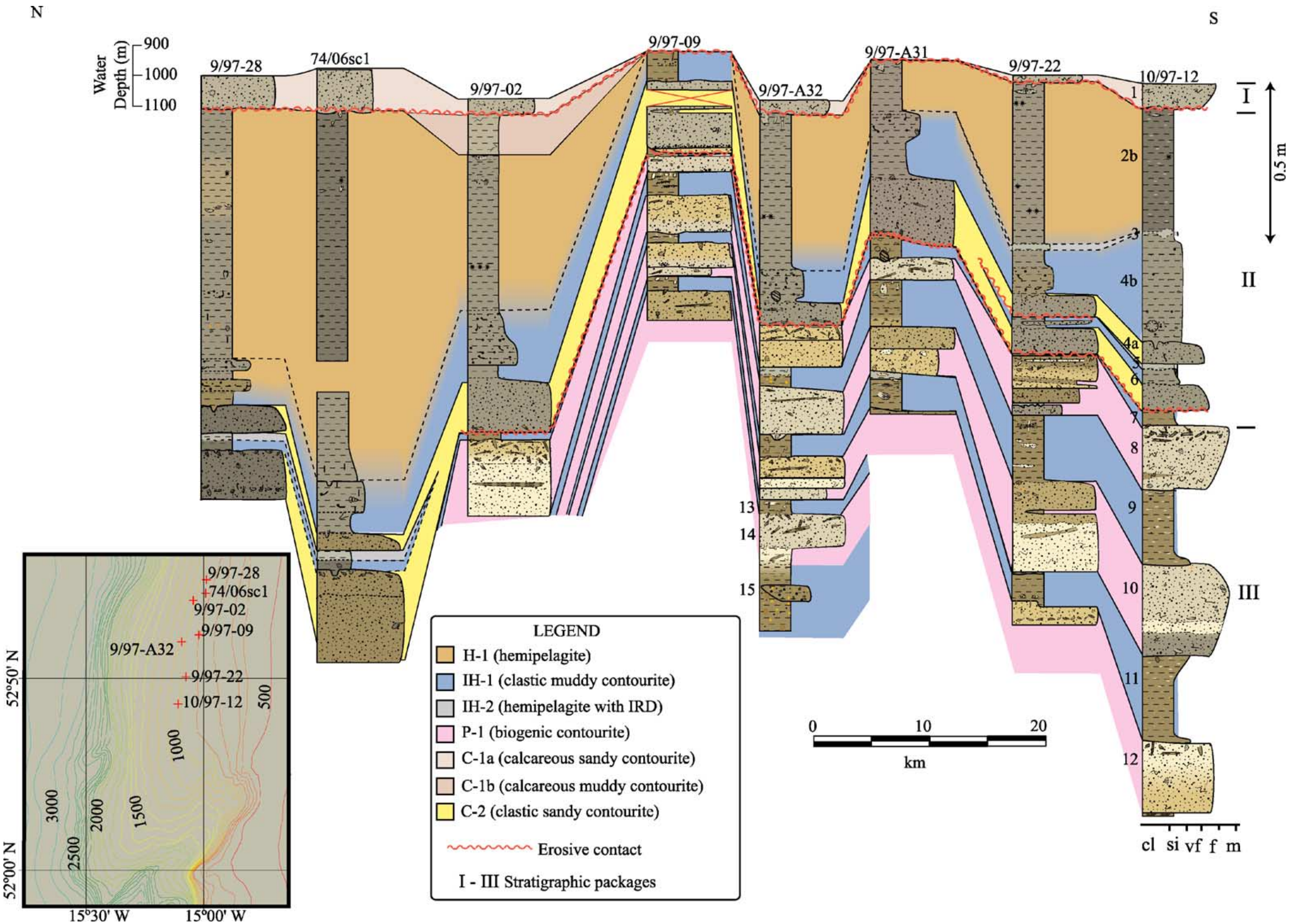

Fig. 9. Transect 1 along upper-slope levels on the west flank of the Porcupine Bank. Stratigraphic units are numbered 1 to 12 and stratigraphic packages I to III downcore.

Table 4
A summary of the stratigraphic units and packages identified on the smooth slope to the west of the Porcupine Bank

Package	Units	Lithofacies make-up	Characteristics	Interpretation
I	1	C-1	Sharp-based, mottled, carbonate-rich mud and sand.	Holocene sandy and muddy contourites.
II	2 (a and b)	IH-1a and H-1	Mud with in situ *Demospongiae* (2a) and clastic-rich mud (2b).	Hemipelagite (2a) at upper slope. Muddy contourite (2b) at mid- and lower slope levels.
	3	IH-1b	Thin, IRD-rich grey, layer.	Hemipelagite with IRD
	4 (a and b)	IH-1a, C-2 and C-3	Sharp-based couplet of graded and occasionally bedded sand (4a) and mud (4b).	Sandy contourite (4a). Muddy contourite (4b).
	5	IH-1b	Thin, IRD-rich grey, layer.	Hemipelagite with IRD.
	6 (a and b)	IH-1, C-2 and C-3	Erosive-based couplet of graded and occasionally bedded sand (6a) and mud (6b).	Sandy contourite (6a). Muddy contourite (6b).
	2	IH-1a	Clastic-rich mud.	Muddy contourite with IRD.
III	8, 10, 12, 14, 16	P-1	Foraminiferal and nannofossil oozes.	Biogenic contourites.
	9, 11, 13, 15, 17	IH-1	Clastic-rich mud.	Muddy contourite with IRD.

pelagic layer (unit 5). Above this layer, there is a second sand–mud couplet (units 4a and 4b) capped by another ice-rafted hemipelagite (unit 3). Two sandy contourite lithofacies (C-2 and C-3) are identified. The structureless C-2 sand was identified at upper- and mid-slope levels (transects 1 and 2; Figs. 9 Figs. 10), while the bedded and occasionally heavily bioturbated and gradationally to sharply-based C-3 facies was deposited at the base of the slope (transect 3). The younger of the sand–mud couplets and a subsequent 'grey band' (lithofacies IH-1b) were followed by the deposition of the muddy unit 2. At mid- and lower-slope levels (Figs. 10 Figs. 11) this mud is relatively sandy and is classified as a muddy contourite (unit 2a; lithofacies IH-1a). On the upper-slope transect (Fig. 9), however, it is less sandy and is interpreted to be a hemipelagite belonging to lithofacies H-1 (unit 2b).

The succession is capped by a calcareous contourite deposit (lithofacies C-1) identified as unit 1 and ascribed to package I. The correlations between cores reveal this package to have an erosive base that can be traced across the slope. This is indicated by the sharp base associated with an enrichment of coarse grains and by thickness variations in the underlying units suggesting that these have been partially or completely removed by erosion (e.g. cores 9/97-09 and 10/97-13). In cores 9/97-09 and 9/97-A31 package I is absent.

At both upper- and mid-slope levels, the stratigraphy is coherent and the succession described above can be identified in all the cores (transects 1 and 2; Figs. 9 Figs. 10). Along the base of the slope, however, the character of the deposits is more variable (transect 3; Fig. 11), although the succession can still be confidently identified in all the cores. Both the mud content and thickness vary along the base of the slope, and in core 9/97-27 the succession was unusually thick and muddy compared to the other cores.

5.1. Sediment composition

Grain counting of two representative cores (83/20sc4 and 83/24sc5), spanning units 1 to 9, reveals detailed profiles (Fig. 12) of the ice-rafted debris (IRD; lithics >150 μm) and foraminifera contents (*N. pachyderma* dextral and sinistral, and *G. bulloides*).

Package I (unit 1) has a low IRD and *N. pachyderma* sinistral content, while *N. pachyderma* dextral and *G. bulloides* are common. The underlying package II (units 2 to 7), on the other hand, has a high but variable IRD content, and *N. pachyderma* sinistral is common to abundant. The two profiled cores show the composition of unit 2 to vary slightly down-slope, as unit 2a (lithofacies H-1; upper slope) has an unusually low IRD-content, whereas the down-slope equivalent unit 2b (lithofacies IH-1; mid-slope levels) has a high IRD-content (up to 14 000 grains/g; Fig. 12). The grain counting also reveals an anomalously high foraminifera content for units 4a and 6a (lithofacies C-2) in package II, and the foraminifera fraction

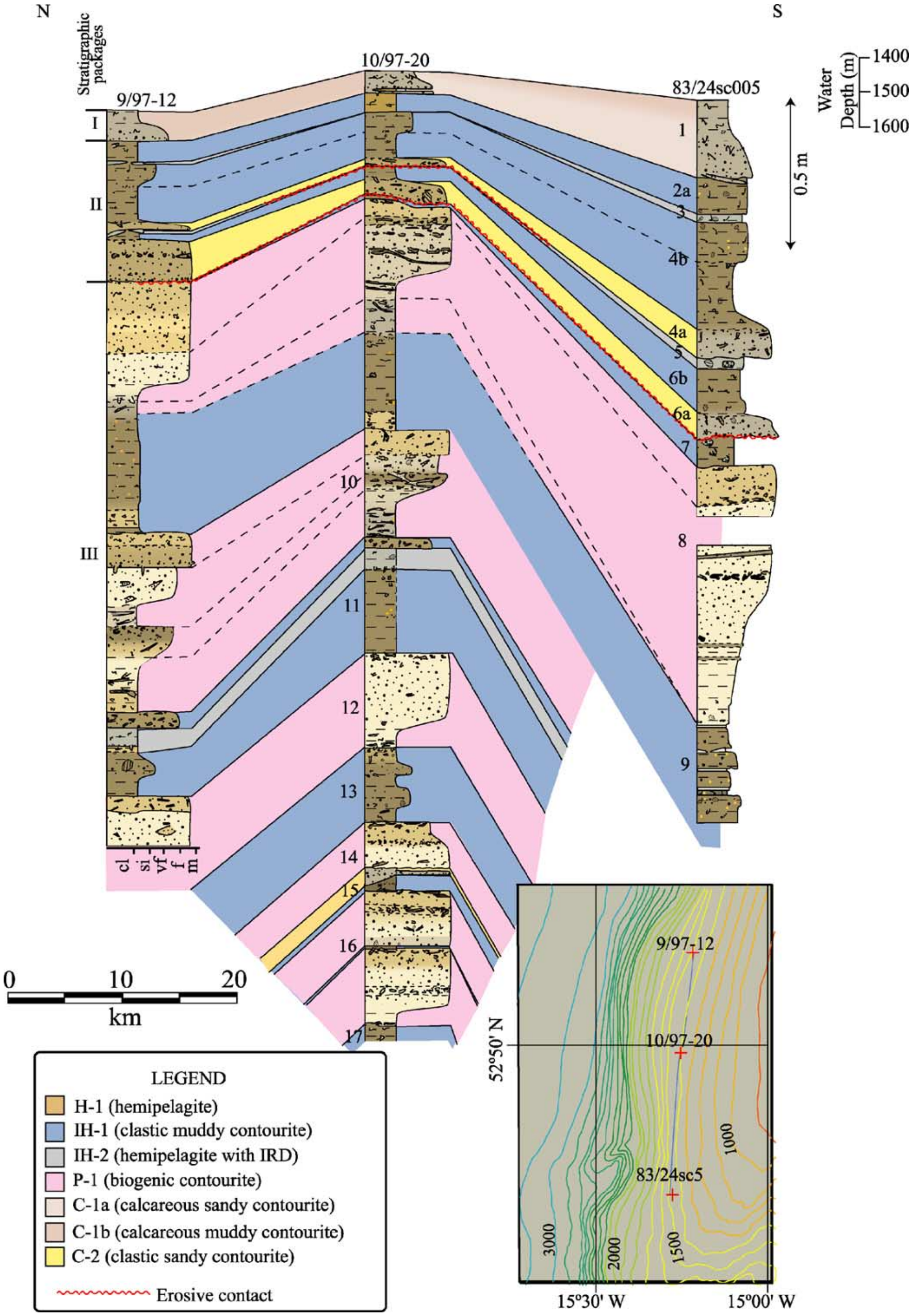

Fig. 10. Transect 2 along mid-slope levels on the west flank of the Porcupine Bank. Stratigraphic units are numbered 1 to 17 and stratigraphic packages I to III downcore.

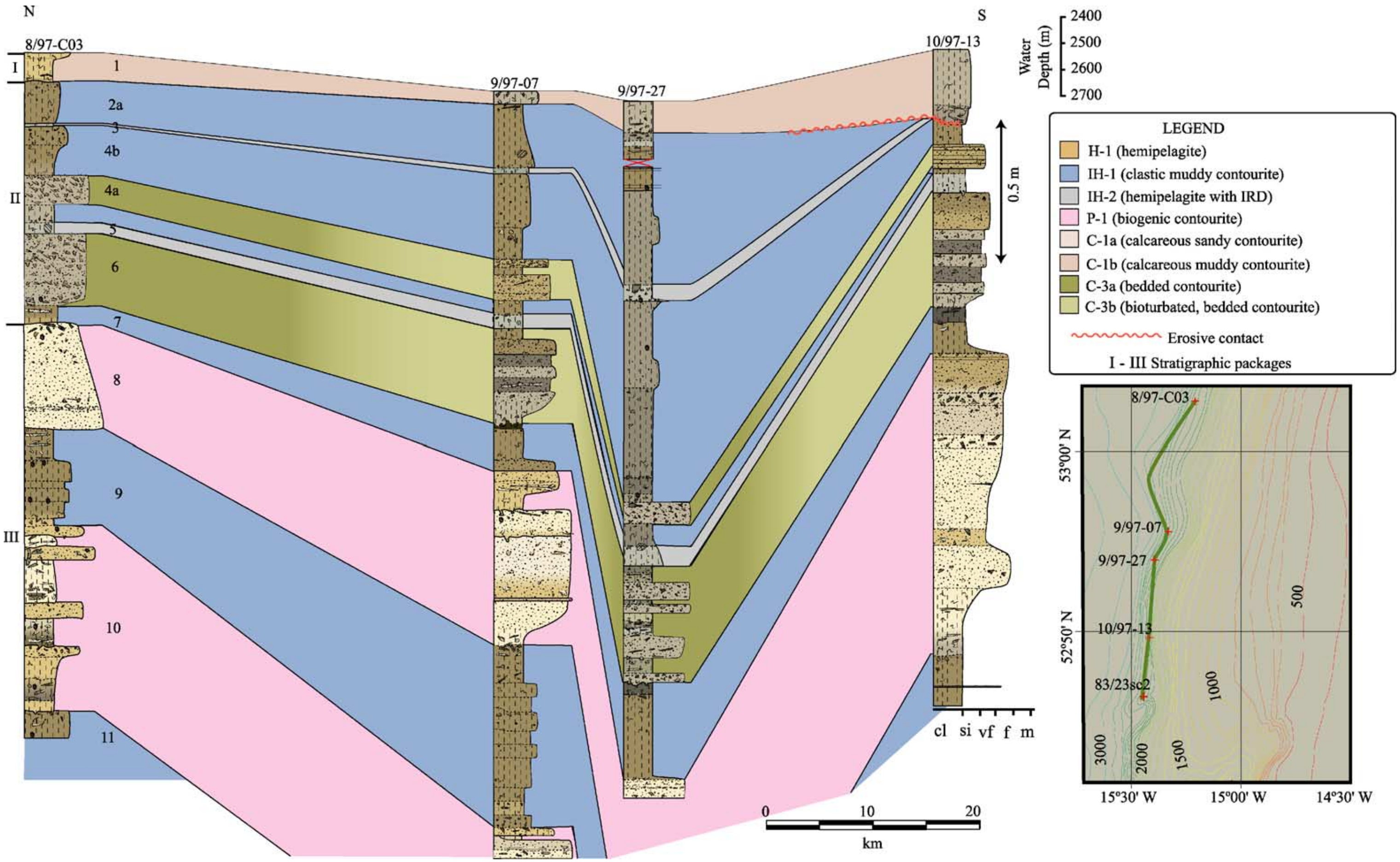

Fig. 11. Transect 3 along lower-slope levels on the west flank of the Porcupine Bank. Stratigraphic units are numbered 1 to 11 and stratigraphic packages I to III downcore.

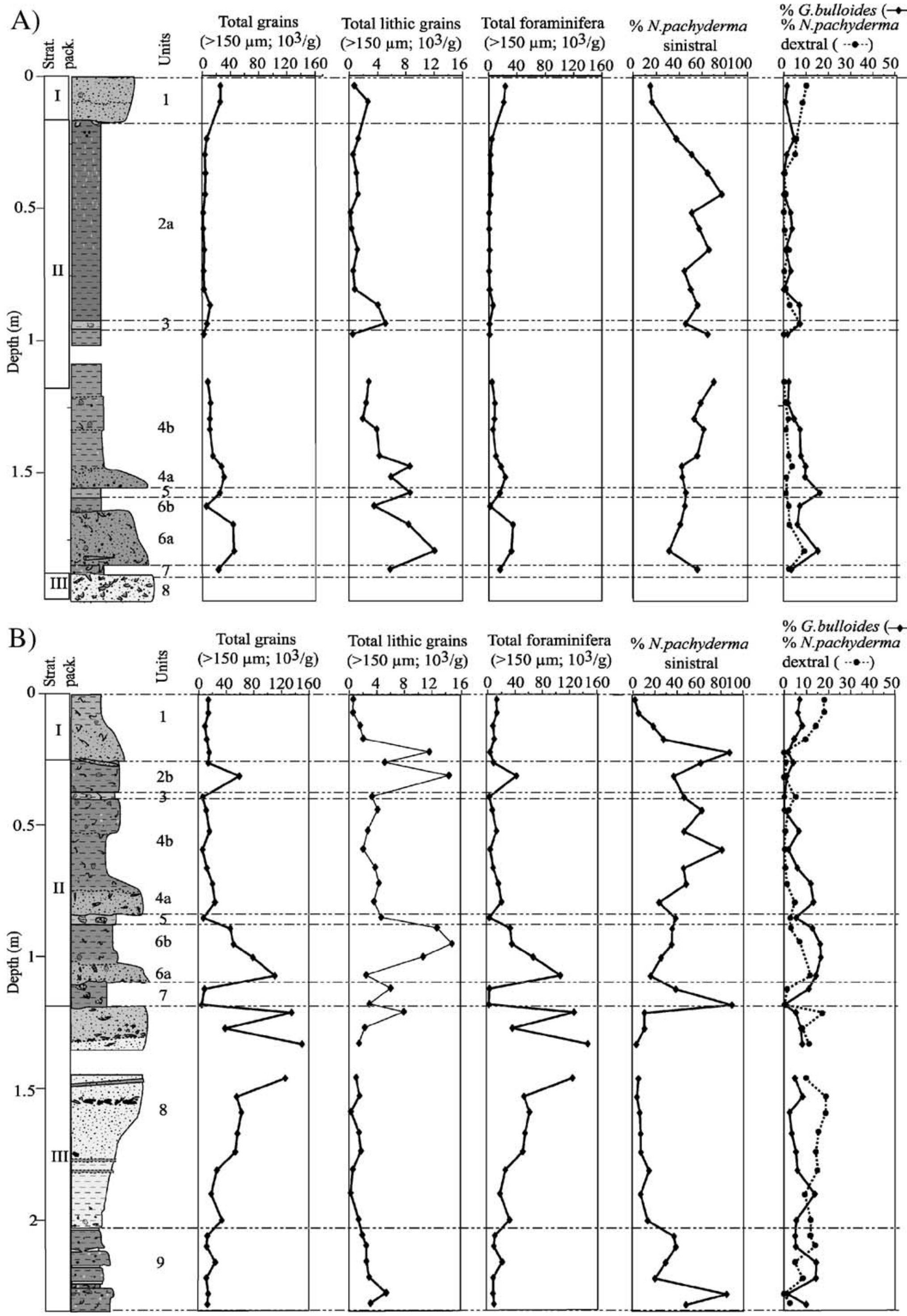

Fig. 12. Detailed profiles showing the downcore distribution of IRD and foraminifera (*G. bulloides* and *N. pachyderma*) resulting from grain counting of cores 83/20sc4 (A) and 83/24sc5 (B).

was dominated by warm and intermediate species (e.g. *G. bulloides* and *N. pachyderma* dextral).

In the underlying package III (units 8 to 17), the biogenic contourite of unit 8 has a low lithic content and a high and diverse foraminifera content (mainly dominated by warm species), while the muddy contourite of unit 9 has a high content of lithics and a corresponding low foraminifera content (Fig. 12).

6. Chronology

Oxygen-isotope profiling is potentially useful for dating purposes (e.g. Bond and Lotti, 1995; Chi and Mienert, 1996), as Marine Isotope Stages (MIS) can be astronomically-tuned and thus dated (Martinson et al., 1987). In the present study, the interpretation of the oxygen-isotope profile for core 83/24sc5 has been used together with AMS ^{14}C dating on bulk samples of planktonic foraminifera in order to establish a chronostratigraphic framework for interpreting the gravity core stratigraphy. The samples selected for dating (Table 5) were also chosen so as to test the lithostratigraphic correlations (Figs. 8–11) and to constrain sedimentation rates. The dating revealed that units 7–17 are beyond the resolution of the ^{14}C technique. For the overlying units (1–6), the ages consistently show a progressively older stratigraphy downcore from ~17 014 cal yrs BP near the top of unit 2 through ~29 172 cal yrs BP near the base of unit 2 to 45 000 cal yrs BP for the top of unit 6 (Table 5). The results confirmed that unit 2a (~17 000–29 000 cal yrs BP) on transect 1 is equivalent to unit 2b (<29 172 cal yrs BP) on transects 2 and 3. The implications of the dating and the sedimentation rates for each stratigraphic package are described further below.

Package I comprising lithofacies C-1 is interpreted as Holocene interglacial contourites resting on a significant erosion surface (see Section 4.4.4). The upper part of package II is revealed to belong to the last glacial by the ^{14}C dating (see Table 5), which is supported by the high content of lithics and cold-water foraminifera (e.g. *N. pachyderma* sinistral). This implies average sedimentation rates of ~2 cm/kyr for units 2 to 6. At upper-slope levels, however, when unit 2 was deposited, the sedimentation rates were relatively high, ~10 cm/kyr in contrast to ~3 cm/kyr further down-slope.

The lower parts of package II are beyond the range of ^{14}C dating (>45 ka) and therefore the timing of these deposits is less uncertain. The carbonate content, down-core variations of *N. pachyderma* and oxygen-isotope profile offer a possible constraint. The oxygen-isotope profile for core 83/24sc5 can be matched to a long $\delta^{18}O$-record obtained by Venz et al. (1999) from ODP site 982 (c. 1100 m water depth) on the Rockall Bank (Fig. 13). This allows the tentative identification of Marine Isotope Stages (MIS) on the Porcupine Bank slope. MIS 1 is equivalent Stratigraphic package I, while package II spans MIS 2 to 5d, the last glacial, consistent with the ^{14}C AMS dates.

The dating of package III is uncertain due to the condensed nature of the succession and as it is beyond

Table 5
Radiometric dating (^{14}C AMS) of gravity cores on the Porcupine Bank where 11 selected samples from package II have been dated (see text for further discussion)

Core	Depth (cm)	^{14}C age	Calibrated age (cal. yr BP)	Calibration data
83/20sc4	30	14 700 ± 70	17 275 (17 014) 16 764	Stuiver et al. (1998)
83/20sc4	87	20 000 ± 120	23 549 (23 113) 22 727	Stuiver et al. (1998)
83/20sc4	116	36 000 ± 270	45 678	Bard (1998)
83/24sc5	48	23 800 ± 80	29 172	Bard (1998)
9/97-09	4	24 000 ± 200	29 429	Bard (1998)
83/24sc3	132	>45 000	>45 000	
83/24sc5	121	>45 000	>45 000	
83/24sc5	183	>45 000	>45 000	
9/97-27	41	15 600 ± 50	18 334 (18 056) 17 782	Stuiver et al. (1998)
9/97-27	86	21 700 ± 70	26 463	Bard (1998)
9/97-27	244	>45 000	>45 000	

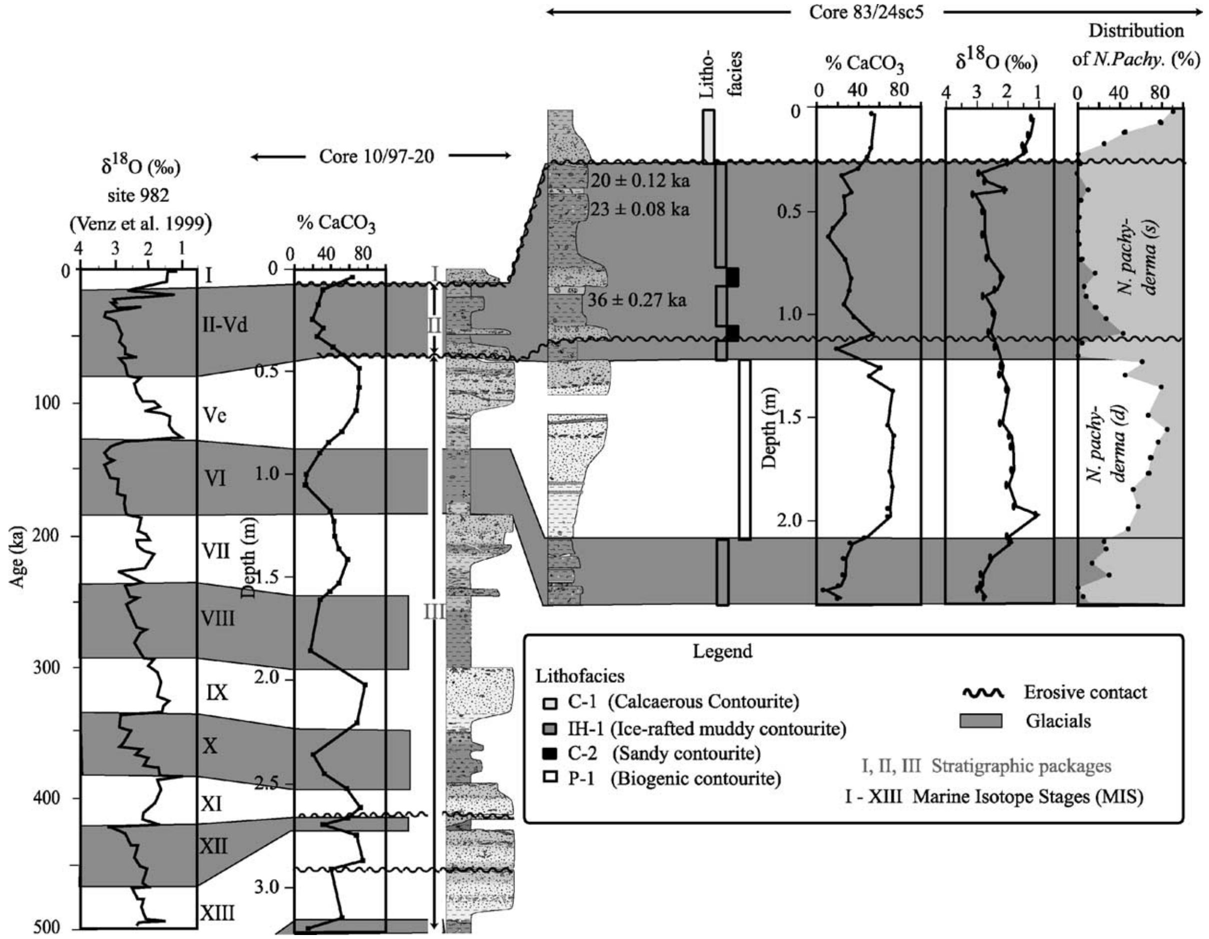

Fig. 13. The depositional events have been timed using AMS radiocarbon (uncorrected C-14 ages) together with oxygen-isotope data (core 83/24sc5), carbonate content (cores 10/97-13, 83/24sc5) and downcore distribution of N. pachyderma (core 83/24sc5). The Oxygen-isotope profile for the core in the present study has been correlated with oxygen-isotope data from ODP site 982. See text for further discussion.

the resolution of the ^{14}C technique. The upper part of package III, the foraminifera ooze (lithofacies P-1), is assigned to the last interglacial, MIS 5e, on the basis of the high carbonate content and the resemblance of the oxygen-isotope profile to that of Venz et al. (1999). Venz et al.'s (1999) data show that regionally light oxygen-isotope values (<1.5) occur only in MIS 1, 5e and possibly 9 (Fig. 13). In the data from core 83/24sc5, the light value (~1) at 2.0 m within the foraminiferal ooze is unlikely to be MIS 9, and therefore MIS 5e is preferred (Fig. 13). The underlying clastic mud deposit (lithofacies IH-1) has a heavy oxygen-isotope value (up to 3), and is therefore ascribed to the previous glacial, MIS 6 which in Venz et al.'s (1999) data has values ranging from ~2.75 to 3.5. These interpretations are supported by the down-core variation of *N. pachyderma*, where sinistral coiling occurs during the glacials and dextral coiling during interglacials (Fig. 13). The results also show that glacials were associated with low carbonate content (average 20%), while interglacials had carbonate contents of up to 75%.

Based on an extrapolation of the carbonate-content pattern downcore, marine isotope stages can be speculatively assigned to the individual units in the longest gravity core record recovered on the Porcupine Bank Slope (core 10/97-20). In this core, MIS 5e-13 are potentially present in package III, revealing an alternation of glacial and interglacial deposition. Interglacial–glacial carbonate variability is a common pattern in the North Atlantic (e.g. Giosan et al., 2002; Grützner et al., 2002; van Weering and de Rijk, 1991; Venz et al., 1999). The full succession cored on the Porcupine Bank slope is thus potentially a record of the last 500 kyr of depositional history (MIS 1 to 13; Fig. 13).

7. Discussion

The coherent shallow stratigraphy that can be traced over an area of at least 1500 km^2 is a record of the depositional history of the slope that can be used to investigate the temporal variations in bottom-current activity, ice-rafting flux and biological productivity during the last glacial cycle and possibly beyond. Importantly, the 3D correlation framework (Figs. 9–11) reveals a number of important features that would not be evident from the study of one core alone. These include two erosive surfaces, the most significant of which occurred within the last glacial (within MIS 3), while the other was cut during the Early Holocene. Other important features include variations in depositional thickness and mud content across and down the slope, indicating variable current strength with time and position. Local enhancements of currents will cause more clay to be suspended resulting in a thinner unit, whereas decreased current strength cause local thickening and more mud-prone units. The stratigraphic correlations also reveal that high on the slope, fine-grained biogenic bottom-current deposits (P-1c and d) are absent (see Section 4.3.1), implying that temporary sediment bypass or erosion took place at upper-slope levels during the penultimate interglacial.

During the last glacial, the distribution of the British–Irish icecap on the shelf and the position of the ice margin are uncertain. However, sedimentation rates on the west Porcupine slope are low, suggesting that glacial melt water did not significantly influence slope sedimentation. Instead the record suggests that the main depositional processes on the Porcupine Bank slope were ice-rafting, pelagic and hemipelagic settling, and bottom currents. The relative importance of these factors was potentially coupled to regional climatic oscillations. Bottom currents can also be influenced by local bathymetric factors such as slope failures, canyons and carbonate mounds. These local controlling factors on the slope sedimentation will be considered first, before the evidence for temporal and spatial variations in bottom-current strength related to regional forcing are considered.

7.1. Bathymetric controls on deposition

The studied part of the Porcupine Bank slope is bounded by a prominent canyon complex to the south and a section of irregular seabed to the north with abundant slope failures and current lineations. Measurements of the modern bottom currents have demonstrated an along-slope steady northward-flow in this area (Dickson and Kidd, 1986). This flow sweeps the entire slope (from 275 to 2354 m) with maximum velocities ranging from 29 cm/s at the base of slope to 37 cm/s on the upper part of the slope (Dickson and McCave, 1986). These current velocities are high enough to cause erosion and winnowing of seabed deposits of clay and silt size (e.g. Black et al., 2003; Southard et al., 1971; van Ledden et al., 2004). The bathymetry data, gravity cores and high-resolution seismic profiles, however, imply that the central smooth slope area has had a history of current deposition, albeit with a relatively condensed contourite accumulation. Several factors might explain the accumulation and preservation of intact, yet condensed, contourites on this part of the slope. The prominent canyon complex to the south might have been instrumental in initiating deposition to the north of it. This is a large feature (up to 20 km wide and 1000 m deep) and northward-directed flow could have experienced a significant momentum loss due to partial deflection of the current and turbulence shedding due to the rough seabed morphology and interactions with deeper water masses in the canyon (Martin White, NUIG, personal communication; Fig. 14). This loss of momentum, coupled with a shallowing of the slope profile north of the canyon, could have forced a deceleration of the current and favoured deposition.

A general thinning of the stratigraphic succession northwards across the area of contourite deposition suggests that either the currents became progressively more sediment depleted or they picked up in strength as they regained the momentum they lost upon passing the canyon. Upon reaching the northern limit of the intact contourite drape, the currents were strong enough to cause lineations at both mid- and upper-

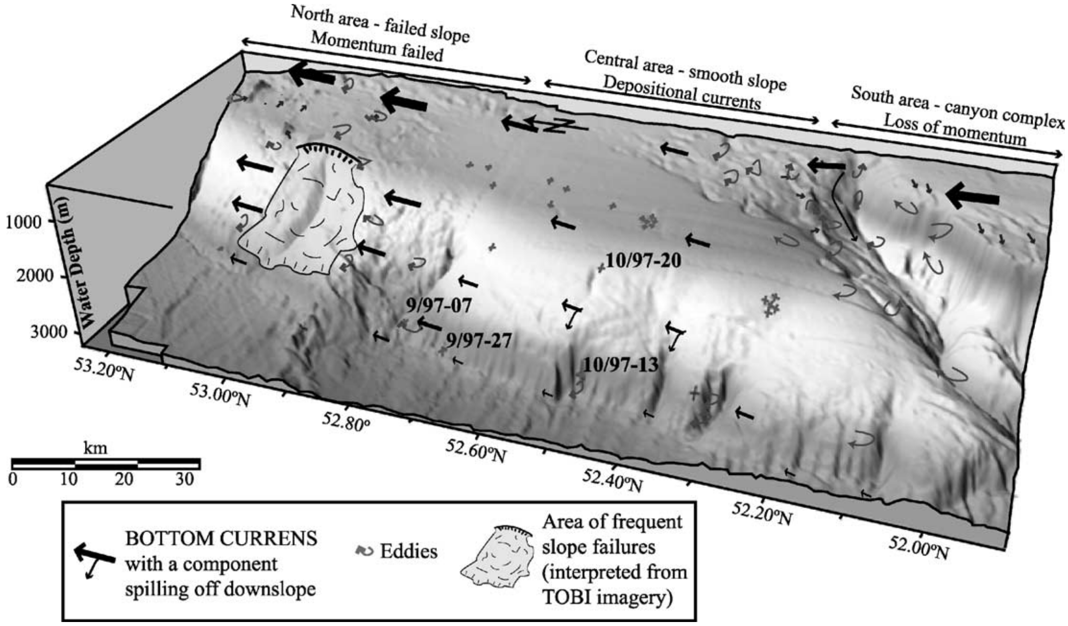

Fig. 14. Model showing how the bathymetry of the Porcupine Bank interacts with the bottom currents. Notice that the canyon complex in the south exhibits an important control on the bottom current, as they loose momentum upon passing these. There is also a possibility of episodic cascading currents down the canyon complex. The location of the three slope areas discussed in the regional setting is also indicated on the figure. (Bathymetry data courtesy of Geological Survey of Ireland.)

slope levels, and to excavate obstacle scours around the carbonate mounds that are found there (the Pelagia Mound Province; Fig. 14). The irregular slope morphology because of increased instability and slope failure would also cause increased turbulence.

At a smaller scale, variations in thickness and structure of the contourite deposits across and down slope might reflect a role for local gradient changes and bathymetric obstacles. A water mass flowing over a steepening slope will have its area of influence decreased and therefore intensify its activity (Howe, 1995; McCave and Tucholke, 1986). Thus the thinning of the stratigraphic succession in core 10/97-20 can be explained by a local increase in the slope gradient to 4° compared to the normal 2°–3° for surrounding areas (Fig. 14).

Current measurements by Dickson and McCave (1986) suggested stronger currents near the top of the Porcupine Bank slope than at the base of the slope. This is in agreement with the gravity-core studies, which identified several erosional surfaces at upper- and mid-slope levels, while at the base of the slope the currents were mostly depositional resulting in thicker deposits without obvious erosional bases. Variations in thickness and character of the deposits along the base of slope, however, imply that local accelerations and decelerations were important. The presence of bedded, sandy contourites in cores 10/97-13 and 9/97-07 indicates strong but variable currents, while the muddy and thickened stratigraphic succession in core 9/97-27 suggests deceleration of currents at this locality. The bathymetry data show the lower parts of the slope are more irregular than that on the upper-slope terrace. Core 10/97-13 (2562 m water depth) coincides with a section of the slope that is irregular and steep (10°–15°). The increased slope gradient would have enhanced bottom currents, while the irregular topography might have increased turbulence. The bedded contourites in core 9/97-07 are located in a wall close to the mouth of a narrow canyon (2 km wide and 250 m deep) that originates at a mid-slope gradient change (c. 2000 m water depth). Canyon mouths are sites of local eddy formation (see Perénne et al., 1997 for example). The turbulent currents combined with local enhancements of velocity might thus account for the presence of bedded contourites in cores 10/97-13 and 9/97-07. More sheltered positions where the currents were less important might explain the mud-prone character of core 9/97-27 as it sits within a depression (50 m deep at 2756 m water depth) at the base-of-slope.

An alternative and more speculative explanation for the presence of the sandy, bedded contourites deep on the slope relates could relate to the bottom-current dynamics at the mid-slope (~1500 m) gradient break. Both bottom and intermediate nepheloid layers with sediment concentrations of 50–150 mg/m^3 (in contrast to 6–25 mg/m^3 for clear water) have been observed on the Goban Spur and along the southern parts of the Porcupine Bank, south of the canyon complex (e.g. McCave et al., 2001; Thorpe and White, 1988). Such nepheloid layers are concentrations of sediment within the water column and are thought to form through erosion of the seabed by internal waves and tides. The present study has shown that episodes of erosion and winnowing recorded at upper- and mid-slope levels (transects 1–2; Figs. 9 and 10) might feed the nepheloid layer increasing its density and possibly causing instability. Additionally, internal waves break on the Porcupine Bank slope (Martin White, NUIG, personal communication). These local instabilities, combined with the sharp break in slope gradients, could result in gravity detachment and episodic spill-off from the mid- and up-slope bottom currents to produce the bedded contourites on the lower slope. In addition, such a mechanism might provide an explanation for the dense array of minor gullies observed on the steep lower slope (Fig. 14).

7.2. Regional climatic controls on deposition

Climatic variation is an important regional control that is closely linked to changes in sea-level, deep-water oceanographic circulation, ice-sheet dynamics and atmospheric conditions (see e.g. Alley and Clark, 1999; Kellogg, 1980; Oppo and Fairbanks, 1990; Raymo et al., 1992; Wang et al., 2002). The local bathymetric controls (described above) are superimposed upon the climatic controls. On the Porcupine Bank slope, Late Quaternary deposition was influenced by biogenic production, intensity of ice-rafting, bottom-current activity and slope instability. Previous work (e.g. Armishaw et al., 2000; Weaver et al., 2000) on contourites has suggested that strong bottom currents are mainly restricted to interglacials, while the bottom currents are absent or weak during glacials. This, however, seems not to be the case for the Porcupine Bank where bottom currents are believed to have been active throughout the depositional history of the slope, with muddy contourites deposited during glacials and sandy contourites during interglacials.

7.2.1. Pre-Midlandian (Stratigraphic package III)

Glacial muddy contourites (lithofacies IH-1a) alternate with interglacial biogenic contourites (lithofacies P-1) in package III. The glacial deposits were the result of a combination of three processes: ice-rafting, hemipelagic settling and bottom currents that were weak to periodically absent. This gave rise to muddy deposits rich in lithic clasts, whereas variations in ice-rafting and in bottom-current activity gave rise to grading of the deposits. The transition from glacial to interglacial conditions was accompanied by decreased ice-rafting and increased bottom-current activity, as recorded by the gradational-based, bioturbated and reverse-graded lithofacies P-1 (Fig. 15A–B). The reverse grading from bioturbated clay to a winnowed but bioturbated sand, conforms with Stow and Piper's (1984) facies model for muddy to sandy contourites. The reverse grading can be explained by a gradual increase in the strength of bottom currents during the interglacial period. At upper-slope levels, however, only the sandier part of the interglacial sandy-contourite is preserved. This may be because either strong currents operated throughout the interglacial at this location, or a waxing current became strong enough to remove the earlier evidence for a flow acceleration. The latter explanation is preferred due to the sharp base at upper-slope levels and occasional internal erosive contacts. The sandy contourites have sharp tops separating them from the overlying muddy contourites (lithofacies IH-1a). This suggests that the transition from interglacial to glacial was accompanied by a sudden drop in bottom-current velocity and an influx of clays and ice-rafted coarser grains.

7.2.2. Midlandian (stratigraphic package II)

The last glacial (MIS Stages 2 to 5d) differs from previous glacials (MIS 6, 8, 10 and 12) in that two periods of increased bottom-current activity were

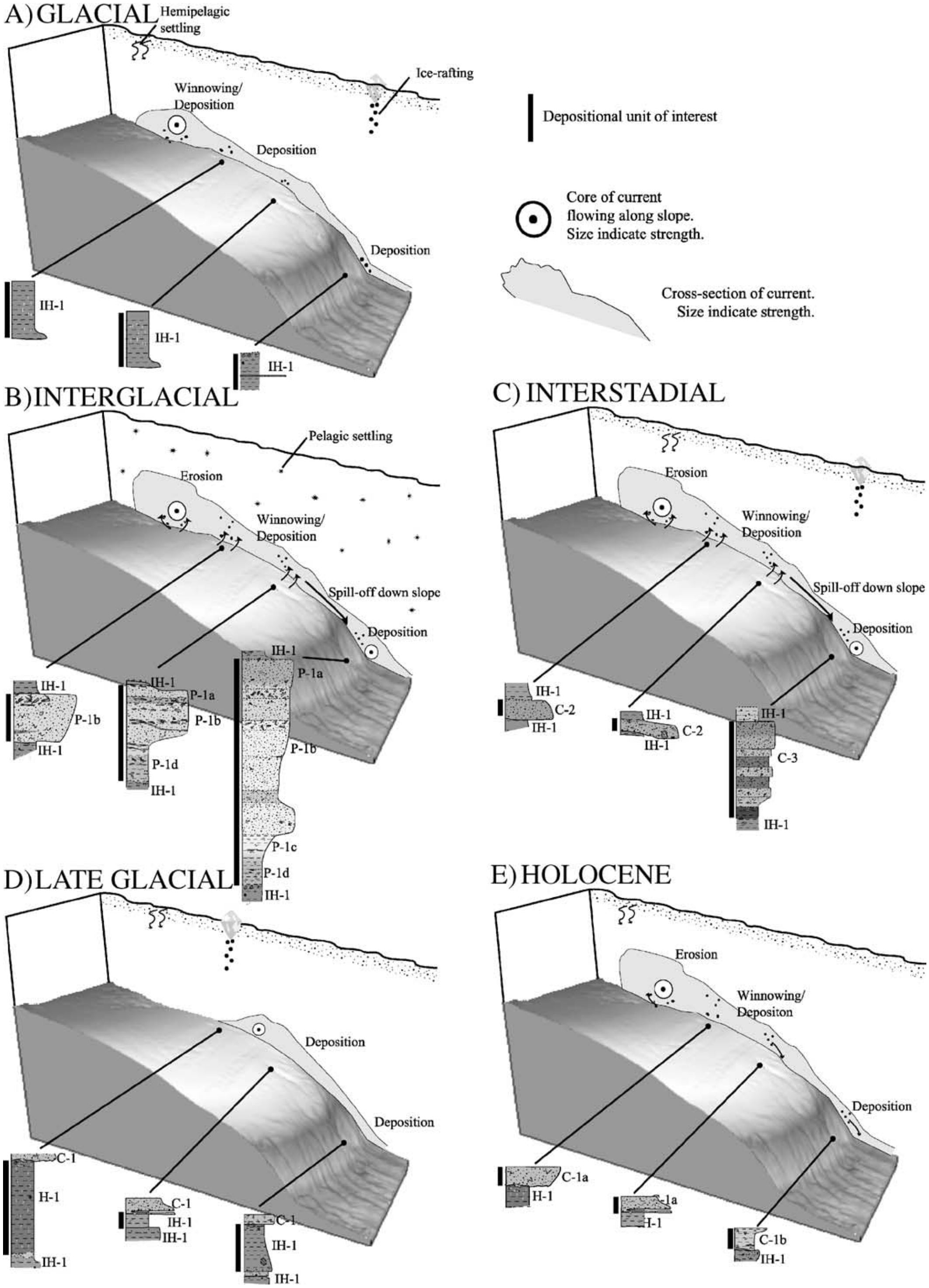

Fig. 15. Model showing how the depositional processes vary with climate and thus time (A–E). It also shows graphic logs of the deposits resulting from the temporal variations of the bottom currents.

recorded within the glacial deposits in the form of the two sandy-muddy contourite couplets (units 4 and 6), most likely within MIS 3. The deposition of the sandy parts of these couplets can be correlated to interstadials. These were characterised by erosive/winnowing currents at upper- and mid-slope levels, while there were strong but variable currents at lower levels giving rise to the bedded sand deposits (lithofacies C-3; Fig. 15C). The first erosional event resulted in the partial or complete removal of the ice-rafted muddy contourites belonging to unit 7 (MIS 4 and possibly early MIS 3 deposits). This erosion was limited to upper- and mid-slope levels, while at base of the slope the deposits are gradationally based, thicker and bedded. This could be explained by weaker bottom currents along the base of the slope with spill-off down-slope of gravity driven density currents (see earlier). After the deposition of these sands (units 4a and 6a) the climate slowly cooled and the current velocity decreased significantly.

During late glacial times (MIS 2) the deposition of muddy contourites continued at lower- and mid-slope levels, while at upper-slope levels no evidence of current activity was recorded (see earlier discussion of lithofacies H-1 and IH-1). The upper slope was instead the site of hemipelagic deposition (unit 2a; lithofacies H-1). This was coeval with the muddy contourites of unit 2b further down the slope, indicating a shift of the core of the current down-slope during late glacial times (Fig. 15D). Shifting of the current core with time was also inferred by van Weering and de Rijk (1991) on the Feni Drift. The shift probably reflects changes in the water mass stratification that controls deep-water circulation. This stratification is controlled by the water mass density, which is a function of salinity and temperature that varied throughout the last glacial (e.g. Adkins et al., 2002; de Vernal and Hillaire-Marcel, 2000; Duplessy et al., 1991). Cooling of the climate as evidenced by a high content of *N. pachyderma* sinistral in unit 2 (Fig. 13) may thus have forced the core of the current deeper on the slope.

7.2.3. Holocene (Stratigraphic package I)

At the glacial / Holocene transition there was a significant warming in the climate. This was associated with enhanced bottom currents and a shifting of the core of the current up-slope again (Fig. 15E) as evidenced by the lithology and sedimentary structures in package I (unit 1). The Holocene deposits (lithofacies C-1) have a sharp to erosive base at upper- and mid-slope levels indicating that, during the Early Holocene, this must have been a site of vigorous bottom currents causing erosion and winnowing of earlier deposits (units 2a and 2b). Along the upper-slope transect, this erosion resulted locally in the complete removal of unit 2 (core 9/97-09). After the erosion sand was deposited along upper- and mid-slope levels, and mud was deposited along the base of the slope. This transition from sand on the upper slope to mud over the lower slope indicates decreasing along-slope current velocities with depth (Fig. 15E).

7.2.4. Regional considerations

Temporal variation of bottom currents linked to changes in climate have been inferred widely across the North Atlantic (e.g. Clark et al., 2002; Dahlgren and Vorren, 2003; Gröger et al., 2003; Howe, 1995; Sierro et al., 1999; Weaver et al., 2000), with stronger currents associated with interglacial warming (e.g. Gröger et al., 2003; Weaver et al., 2000). However, bottom currents were also important, albeit weaker, during glacial times. The existence of active glacial bottom currents within the Rockall Trough is in agreement with Knutz et al.'s (2001, 2002a) studies of the distal Barra Fan. Further north, outside of the Rockall Trough, glacial bottom-current activity has also been reported, as Laberg and Vorren (2004) recorded a slope contourite which was active during the last glacial offshore Norway.

The last glacial period was characterised by periods of interstadial warming during MIS 3, and these were accompanied by waxing and waning of bottom currents on the Porcupine Bank. Elsewhere in the Rockall Trough, the record of interstadial strong bottom currents is limited, but Knutz et al. (2002b) recorded contourite deposition within interstadials on the Barra Fan on the eastern margin of the Rockall Trough. This, together with the results of the present study, could indicate that interstadial warming of the climate, at least during the last glacial episode, was linked to transient strengthening in the bottom-current activity along the eastern margins of the Rockall Trough.

The Barra Fan was also the site of extensive bottom-current activity during the Holocene (e.g. Akhurst, 1991; Armishaw et al., 2000; Howe, 1996;

Howe et al., 1998; Knutz et al., 2001, 2002a,b). Armishaw et al. (2000) identified erosive-based sandy contourites that they interpreted as the result of strong, erosive bottom currents during the Early Holocene. Present-day strong bottom currents have also been reported south of the study area, on the Goban Spur, by van Weering et al. (2001). In this area, the bottom currents are at present strongest along the shelf edge and upper-slope where resuspension and transport of sediment is occurring. Further down the slope on the Goban Spur the environment is more favourable for deposition of suspended matter as the currents are weaker there (Thomsen and van Weering, 1998; van Weering et al., 2001). These observations of the present day conditions on the Goban Spur are similar to the interpretations of the Holocene deposits on the Porcupine Bank.

8. Conclusions

The cored stratigraphy on an area of smooth slope west of Porcupine Bank demonstrates an alternation between clastic (glacial) and carbonate-rich (interglacial) deposits that can be correlated across an area of at least 1500 km^2. The sedimentological study of the cores has confirmed the presence of active bottom currents on a sediment-starved slope as evidenced by winnowed sandy contourites, muddy contourites, laterally extensive erosive surfaces, and current lineations recorded on TOBI side-sonar imagery. The strength, location and direction of the bottom currents were controlled by both regional (climate) and local factors (seabed topography). The distinction between regional and local controls was facilitated by the use of a network of correlated cores, rather than a single core. The main results from the study are as follows:

1. Bottom currents are strong on the Porcupine Bank slopes as indicated by a rough morphology with carbonate mounds, moats, slope failures and abundant current lineations. Between 52°15′N and 52°45′N the slope is, however, smooth with no current lineations, and a near continuous, but condensed depositional record, possibly as old as 500 kyr, is preserved here. The deposition and preservation of this record can be explained by a reduction in current strength attributed to the presence of a prominent canyon complex in the south, as there would have been a considerable loss in flow momentum as the currents passed this canyon. The bottom currents were also locally enhanced upon encountering bathymetric obstacles such as carbonate mounds.
2. Bottom currents to the west of Porcupine Bank were generally strong during interglacials and interstadials, whereas they were weak during stadials. During the last glacial, significant enhancement of the bottom currents took place at least twice and these can be correlated to interstadial warming of the climate within MIS 3. During this time erosion and winnowing of previous stadial deposits occurred at upper- and middle-slope levels.
3. The climate also played an important role on the positioning of the core of the current. A significant shift occurred during the late glacial when the core of the current was present at mid-slope levels (1200–2300 m) while today it is at upper-slope levels (500–1200 m).
4. The results of the sedimentary study showed that bottom-current activity during the last glacial was significantly different to previous glacials when no comparable interstadial bottom-current episodes have been identified. In addition, previous interglacial deposits record periods of increasing bottom currents resulting in reverse-graded calcareous oozes. The Holocene interglacial, on the other hand, preserves evidence of stronger currents at the start of the period than today, and the Holocene deposits have a mixed calcareous and terrigenous composition. The reason for the differences between the last glacial and previous glacials and between the Holocene interglacial and previous interglacials is unclear, and more work is needed to explain these observations.

Acknowledgements

This project has been funded by the Offshore Support Group (OSG) and the Rockall Studies (RSG) Group of the Irish Petroleum Infrastructure Programme Group 2 which was established by the Petroleum Affairs Division of the Department of the Marine and Natural Resources on 4 June, 1997 in conjunction with the award of exploration licences under the Rockall Trough Frontier Licensing Round. The RSG comprised: Agip (UK) Ltd, Anadarko Ireland Company, ARCO Ireland Offshore Inc, BG Exploration and Production Ltd, BP Exploration Operating Company Ltd, British–Borneo International Ltd, Elf Petroleum Ireland BV, Enterprise Oil plc, Mobil North Sea Ltd, Murphy Offshore Ireland Ltd, Phillips Petroleum Exploration Ireland Ltd, Saga Petroleum Ireland Ltd, Shell EP Ireland B.V., Statoil Exploration (Ireland) Ltd, Total Oil Marine plc, Union Texas Petroleum Ltd and the Petroleum Affairs Division of the Department of the Marine and Natural Resources. The paper also uses data and survey results from the marine seabed survey acquired for the Geological Survey of Ireland (GSI). The authors would specifically like to thank Eibhlín Doyle and Xavier Monteys of the GSI for data and discussions. We would also like to thank Martin White at NUI Galway for helpful discussions on oceanography and Jean Vacelet at Centre d'Oceanographie de Marseille for help in identifying sponge spicules. Finally we would like to thank referees and editor for helpful comments and suggestions.

References

Abrantes, F., Baas, J., Haflidason, H., Rasmussen, T., Klitgaard, D., Loncaric, N., Gaspar, L., 1998. Sediment fluxes along the northeastern European Margin: inferring hydrological changes between 20 and 8 kyr. Mar. Geol. 152, 7–23.

Adkins, J.F., McIntyre, K., Schrag, D.P., 2002. The salinity, temperature and $\delta^{18}O$ of the glacial deep ocean. Science 298, 1769–1773.

Akhurst, M.C., 1991. Aspects of Late Quaternary sedimentation in the Faroe–Shetland Channel, Northwest UK continental margin. BGS Technical Report, WB/91/2.

Alley, R.B., Clark, P.U., 1999. The deglaciation of the Northern Hemisphere: a global perspective. Annu. Rev. Earth Planet. Sci. 27, 149–182.

Armishaw, J.E., Holmes, R.W., Stow, D.A.V., 2000. The Barra Fan: a bottom-current reworked, glacially-fed submarine fan system. Mar. Pet. Geol. 17, 219–238.

Bard, E., 1998. Geochemical and geophysical implications of the radiocarbon calibration. Geochim. Cosmochim. Acta 62 (12), 2025–2038.

Black, K.S., Peppe, O.C., Gust, G., 2003. Erodibility of pelagic carbonate ooze in the northeast Atlantic. J. Exp. Mar. Biol. Ecol. 285–286, 143–463.

Boldreel, L.O., Andersen, M.S., 1995. The relationship between the distribution of Tertiary sediments, tectonic processes and deep-water circulation around the Faeroe Islands. In: Tudhope, A.W. (Ed.), The Tectonics, Sedimentation and Palaeoceanography of the North Atlantic Region. Geological Society, London, pp. 145–158.

Bond, G., Lotti, R., 1995. Iceberg discharge into the North Atlantic on millennial time scales during the last glaciation. Nature 267, 1005–1010.

Bond, G., Heinrich, H., Broecker, W., Labeyrie, L., McManus, J., Andrews, J., Huon, S., Jantschick, R., Clasen, S., Simet, C., Tedesco, K., Klas, M., Bonanin, G., Ivy, S., 1992. Evidence for massive discharges of icebergs into the North Atlantic Ocean during the last glacial period. Nature 360, 245–248.

Bowen, D.Q., Rose, J., McCabe, A.M., Sutherland, D.G., 1986. Correlation of Quaternary glaciations in England, Ireland, Scotland and Wales. Quat. Sci. Rev. 5, 299–340.

Bowen, D.Q., Phillips, F.M., McCabe, A.M., Knutz, P.C., Sykes, G.A., 2002. New data for the last glacial maximum in Great Britain and Ireland. Quat. Sci. Rev. 21, 89–101.

Chi, J., Mienert, J., 1996. Linking physical property records of Quaternary sediments to Heinrich events. Mar. Geol. 131, 57–73.

Clark, P.U., Pisias, N.G., Stocker, T.F., Weaver, A.J., 2002. The role of the thermohaline circulation in abrupt climate change. Nature 415, 863–869.

Coxon, P., 2001. Cenozoic: Tertiary and Quaternary (until 10,000 years before present). In: Holland, C.E. (Ed.), The Geology of Ireland. Dunedin Academic Press, Edinburgh, pp. 387–427.

Cremer, M., Faugères, J.-C., Grousset, F., Gonthier, E., 1993. Late Quaternary sediment flux on sedimentary drifts in the Northeast Atlantic. Sediment. Geol. 82, 89–101.

Dahlgren, K.I.T., Vorren, T.O., 2003. Sedimentary environment and glacial history during the last 40 ka of the Vøring continental margin, mid-Norway. Mar. Geol. 193, 93–127.

Davies, R., Cartwright, J., Pike, J., Line, C., 2001. Early Oligocene initiation of North Atlantic Deep Water formation. Nature 410, 917–920.

de Vernal, A., Hillaire-Marcel, C., 2000. Sea-ice cover, sea-surface salinity and halo-thermocline structure of the northwest North Atlantic: modern versus full glacial conditions. Quat. Sci. Rev. 19 (1–5), 65–85.

Dickson, R.R., Kidd, R.B., 1986. Deep circulation in the southern Rockall Trough—the oceanographic setting of site 610. In: Ruddiman, W.F., Kidd, R.B., Thomas, E., et al., (Eds.), Initial Reports Deep-Sea Drilling Project, Washington, pp. 1061–1073.

Dickson, R.R., McCave, I.N., 1986. Nepheloid layers on the continental slope west of Porcupine Bank. Deep-Sea Res. 33, 791–818.

Dowling, L.M., McCave, I.N., 1993. Sedimentation on the Feni Drift and late glacial bottom water production in the northern Rockall Trough. Sediment. Geol. 82, 79–87.

Duplessy, J.-C., Labeyrie, L., Juillet-Lecrec, A., Maitre, F., Duprat, J., Sarnthein, M., 1991. Surface salinity reconstruction of the North Atlantic Ocean during last glacial maximum. Oceanol. Acta 14 (4), 311–324.

Ellett, D.J., Martin, J.H.A., 1973. The physical and chemical oceanography of the Rockall Channel. Deep-Sea Res. I 20, 585–625.

Ellett, D.J., Edwards, A., Bowers, R., 1986. The hydrography of the Rockall Channel—an overview. Proc. R. Soc. Edinb. 88B, 61–81.

Elliot, M., Labeyrie, L., Duplessy, J.-C., 2002. Changes in North Atlantic deep-water formation associated with the Dansgaard–Oeschger temperature oscillations (60–10 ka). Quat. Sci. Rev. 21, 1153–1165.

Games, K.P., 2001. Evidence of shallow gas above the Connemara oil accumulation, Block 26/28, Porcupine Basin. In: Shannon, P.M., Haughton, P.D.W., Corcoran, D.V. (Eds.), The Petroleum Exploration of Ireland's Offshore Basins, Special Publication-Geological Society of London, pp. 361–373.

Giosan, L., Flood, R.D., Grützner, J., Mudie, P., 2002. Paleoceanographic significance of sediment color on western North Atlantic Drifts: II. Late Pliocene–Pleistocene sedimentation. Mar. Geol. 189, 43–61.

Gröger, M., Henrich, R., Bickert, T., 2003. Glacial–interglacial variability in lower North Atlantic deep water: inference from silt grain-size analysis and carbonate preservation in the western equatorial Atlantic. Mar. Geol. 201, 321–332.

Grützner, J., Giosan, L., Franz, S.O., Tiedemann, R., Cortijo, E., Chaisson, W.P., Flood, R.D., Hagen, S., Keigwin, L.D., Poli, S., Rio, D., Williams, T., 2002. Astronomical age models for Pleistocene drift sediments from the western North Atlantic (ODP Sites 1055–1063). Mar. Geol. 189, 5–23.

Haughton, P., Praeg, D., Shannon, P., Garrington, G., Higggs, K., Amy, L., Tyrrell, S., Morrissey, T., 2005. First results from shallow stratigraphic boreholes on the eastern flank of the Rockall Basin, offshore western Ireland. In: Doré, A.G., Vining, B. (Eds.), Petroleum Geology: North-West Europe and Global Perspectives - Proceedings of the 6th Petroleum Geology Conference. Geological Society, London, pp. 1077–1094.

Heinrich, H., 1988. Origin and consequences of cyclic ice rafting in the northeast Atlantic Ocean during the past 130,000 years. Quat. Res. 29, 142–152.

Holliday, N.P., Pollard, R.T., Read, J.F., Leach, H., 2000. Water mass properties and fluxes in the Rockall Trough, 1975–1998. Deep-Sea Res. I 47, 1303–1332.

Howe, J.A., 1995. Sedimentary processes and variations in slope–current activity during the last glacial–interglacial episode on the Hebrides Slope, northern Rockall Trough, North Atlantic Ocean. Sediment. Geol. 96, 201–230.

Howe, J.A., 1996. Turbidite and contourite sediment waves in the northern Rockall Trough, North Atlantic Ocean. Sedimentology 43, 219–234.

Howe, J.A., Harland, R., Hine, N.M., Austin, W.E.N., 1998. Late Quaternary stratigraphy and palaeoceanographic change in the northern Rockall Trough, North Atlantic Ocean. In: Stoker, M.S., Evans, D., Cramp, A. (Eds.), Geological Processes on Continental Margins: Sedimentation, Mass-Wasting and Stability, Special Publication-Geological Society of London, pp. 269–286.

Huthnance, J.M., 1986. The Rockall slope current and shelf-edge processes. Proc. R. Soc. Edinb. 88B, 83–101.

Kellogg, T.B., 1980. Paleoclimatology and paleo-oceanography of the Norwegian and Greenland seas: glacial–interglacial contrasts. Boreas 9, 115–137.

Kenyon, N.H., Akhmetzhanov, A.M., Wheeler, A.J., van Weering, T.C.E., de Haas, H., Ivanov, M.K., 2003. Giant carbonate mud mounds in the southern Rockall Trough. Mar. Geol. 195, 5–30.

Knutz, P.C., Austin, W.E.N., Jones, E.J.W., 2001. Millennial-scale depositional cycles related to British Ice Sheet variability and North Atlantic paleocirculation since 45 kyr B.P., Barra Fan, U.K. margin. Paleoceanography 16 (1), 53–64.

Knutz, P.C., Jones, E.J.W., Austin, W.E.N., van Weering, T.C.E., 2002a. Glacimarine slope sedimentation, contourite drifts and bottom current pathways on the Barra Fan, UK North Atlantic margin. Mar. Geol. 188 (129-146).

Knutz, P.C., Jones, E.J.W., Howe, J.A., van Weering, T.C.E., Stow, D.A.V., 2002b. Wave-formed sheeted contourite drift on the Barra Fan, NW UK continental margin. In: Stow, D.A.V., Pudsey, C.J., Howe, J.A., Faugères, J.-C., Viana, A.R. (Eds.), Deep-Water Contourite Systems: Modern Drifts and Ancient Series, Seismic and Sedimentary Characteristics, Memoirs of the Geological Society of London, pp. 85–97.

Laberg, J.S., Vorren, T.O., 2004. Weichselian and Holocene growth of the northern high-latitude Lofoten contourite drift on the continental slope of Norway. Sediment. Geol. 164 (1–17).

Labeyrie, L., Leclaire, H., Waelbroeck, C., Cortijo, E., Duplessy, J.-C., Vidal, L., Elliot, M., Le Coat, B., Auffret, G., 1999. Temporal variability and deep waters of the North West Atlantic Ocean at orbital and millennial scales. In: Clark, P.U., Webb, R.S., Keigwin, L.D. (Eds.), Mechanisms of Global Climate Change at Millennial Time Scales. Geophysical Monograph, pp. 77–98.

Lagerklint, I.M., Wright, J.D., 1999. Late glacial warming prior to Heinrich event: 1. The influence of ice-rafting and large ice sheets on the timing of initial warming. Geology 27, 1099–1102.

Martinson, D.G., Pisias, N.G., Hays, J.D., Imbrie, J., Moore, T.C., Shackleton, N.J., 1987. Age dating and the orbital theory of the ice-ages: development of a high-resolution 0 to 300,000-year chronostratigraphy. Quat. Res. 27, 1–29.

Masson, D.G., Howe, J.A., Stoker, M.S., 2002. Bottom-current sediment waves, sediment drifts and contourites in the northern Rockall Trough. Mar. Geol. 192, 215–237.

McCartney, M.S., Mauritzen, C., 2001. On the origin of the warm inflow to the Nordic Seas. Prog. Oceanogr. 51, 125–214.

McCave, I.N., Tucholke, B.E., 1986. Deep-current controlled sedimentation in the western North Atlantic. In: Vogt, P.R., Tucholke, P.R. (Eds.), The Geology of Western North America, vol. M. The western North Atlantic Region. Geological Society of America, Boulder, Colorado, pp. 1117–1126.

McCave, I.N., Hall, A.M., Anita, A.N., Chou, L., Dehairs, F., Lampitt, R.S., Thomsen, L., van Weering, T.C.E., Wollast, R., 2001. Distribution, composition and flux of particulate material over the European margin at 47°–50°N. Deep-Sea Res. II 48, 3107–3139.

Müller, G., 1967. Methods in sedimentary petrology. E. Scweizerbart'sche Verlagsbuchhandlung (283 pp.).

New, A.L., Smythe-Wright, D., 2001. Aspects of the circulation in the Rockall Trough. Cont. Shelf Res. 21, 777–810.

New, A.L., Barnard, S., Herrmann, P., Molines, J.-M., 2001. On the origin and pathways of the saline inflow to the Nordic Seas: insight from models. Prog. Oceanogr. 48, 255–287.

Oppo, D.W., Fairbanks, R.G., 1990. Atlantic ocean thermohaline circulation of the last 150,000 years: relationship to climate and atmospheric CO_2. Paleoceanography 5 (3), 277–288.

O'Reilly, B.M., Readman, P.W., Shannon, P.M., 2001. TRIM, TOBI Rockall Irish Margins. Final Report. Rockall Studies Group Report, Project 97/14a.

O'Reilly, B.M., Readman, P.W., Shannon, P.M., Jacob, A.W.B., 2003. A model for the development of a carbonate mound population in the Rockall Trough based on deep-towed sidescan sonar data. Mar. Geol. 198, 55–66.

Perénne, N., Verron, J., Renouard, D., Boyer, D.L., Zhang, X., 1997. Rectified barotropic flow over a submarine canyon. J. Phys. Oceanogr. 27, 1868–1893.

Pollard, R.T., Griffiths, M.J., Cunningham, S.A., Read, J.F., Pérez, F.F., Rios, A.F., 1996. Vivaldi 1991 — a study of the formation, circulation and ventilation of Eastern North Atlantic Central Water. Prog. Oceanogr. 37, 167–192.

Raymo, M.E., Hodell, D.A., Jansen, E., 1992. Response of deep ocean circulation to initiation of Northern Hemisphere glaciation (2–3 Ma). Paleoceanography 7 (5), 645–672.

Read, J.F., 2001. CONVEX-91: water masses and circulation of the Northeast Atlantic subpolar gyre. Prog. Oceanogr. 48, 461–510.

Scoffin, T.P., Bowes, G.E., 1988. The facies distribution of carbonate sediments on Porcupine Bank, northeast Atlantic. Sediment. Geol. 60, 125–134.

Shackleton, N.J., Backmann, J., Zimmermann, H., Kent, D.V., Hall, M.A., Roberts, D.G., Schnitker, D., Baldauf, J., Desprairies, A., Homrighausen, R., Huddlestun, P., Keene, J.B., Kaltenback, A.J., Krumsieck, K.A.O., Morton, A.C., Murray, J.W., Westberg-Smith, J., 1984. Oxygen isotope calibration of the onset of ice-rafting and history of glaciation in the North Atlantic region. Nature 307, 620–623.

Sierro, F.J., Flores, J.A., Baraza, J., 1999. Late glacial to recent paleoenvironmental changes in the Gulf of Cadiz and formation of sandy contourite layers. Mar. Geol. 155, 157–172.

Southard, J.B., Young, R.A., Hollister, C.D., 1971. Experimental erosion of calcareous ooze. J. Geophys. Res. 76, 5903–5909.

Stoker, M.S., 1997. Mid to late Cenozoic sedimentation on the continental margin off NW Britain. J. Geol. Soc. London 154, 509–515.

Stoker, M.S., van Weering, T.C.E., Svaerdborg, T., 2001. A mid to late Cenozoic tectonostratigraphic framework for the Rockall Trough. In: Shannon, P.M., Haughton, P.D.W., Corcoran, D.V. (Eds.), The Petroleum Exploration of Ireland's Offshore Basins, Special Publication-Geological Society of London, pp. 411–438.

Stoker, M.S., Praeg, D., Shannon, P.M., Hjelstuen, B.O., Laberg, J.S., van Weering, T.C.E., Sejrup, H.P., Evans, D., 2005. Neogene evolution of the Atlantic continental margin of NW Europe (Lofoten Islands to SW Ireland): anything but passive. In: Doré, A.G., Vining, B. (Eds.), Petroleum Geology: North-West Europe and Global Perspectives—Proceedings of the 6th Petroleum Geology Conference. Geological Society, London, pp. 1057–1076.

Stow, D.A.V., Holbrook, J.A., 1984. North Atlantic contourites: an overview. In: Stow, D.A.V., Piper, D.J.W. (Eds.), Fine Grained Sediments: Deep Water Processes and Facies, Special Publication-Geological Society of London, pp. 245–256.

Stow, D.A.V., Piper, D.J.W., 1984. Deep-water fine-grained sediments: facies models. In: Stow, D.A.V., Piper, D.J.W. (Eds.), Fine Grained Sediments: Deep Water Processes and Facies, Special Publication-Geological Society of London, pp. 611–646.

Stow, D.A.V., Tabrez, A.R., 1998. Hemipelagites: processes, facies and models. In: Stoker, M.S., Evans, D., Cramp, A. (Eds.), Geological Processes on Continental Margins: Sedimentation, Mass-Wasting and Stability, Special Publication-Geological Society of London, pp. 317–337.

Stow, D.A.V., Faugères, J.-C., Howe, J.A., Pudsey, C.J., Viana, A.R., 2002. Bottom currents, contourites and deep-sea sediment drifts: current state-of-the-art. In: Stow, D.A.V., Pudsey, C.J., Howe, J.A., Faugères, J.-C., Viana, A.R. (Eds.), Deep-Water Contourite Systems: Modern Drifts and Ancient Series, Seismic and Sedimentary Characteristics, Memoirs of the Geological Society of London, pp. 7–20.

Stuiver, M., Reimer, P.J., 1993. Extended ^{14}C data base and revised CALIB 3.0 ^{14}C age calibration program. Radiocarbon 35 (1), 215–230.

Stuiver, M., Reimer, P.J., Bard, E., Beck, W., Burr, G.S., Hughen, K.A., Kromer, B., McCormac, G., van der Plicht, J., Spurk, M., 1998. INTCAL 98 radiocarbon age calibration, 24,000–0 cal BP. Radiocarbon 40 (3), 1041–1083.

Talley, L.D., McCartney, M.S., 1982. Distribution and circulation of Labrador Sea Water. J. Phys. Oceanogr. 12, 1189–1205.

Thomsen, L., van Weering, T.C.E., 1998. Spatial and temporal variability of particulate matter in the benthic boundary layer at the N.W. European Continental Margin (Goban Spur). Prog. Oceanogr. 42, 61–76.

Thorpe, S.A., White, M., 1988. A deep intermediate nepheloid layer. Deep-Sea Res., A, Oceanogr. Res. Pap. 9, 1665–1671.

Tucholke, B.E., Mountain, G.S., 1986. Tertiary paleoceanography of the western North Atlantic Ocean. In: Tucholke, B.E. (Ed.), The Geology of North America, volume M. The Western North Atlantic Region. Geological Society of America, Boulder, CO, pp. 631–650.

Unnithan, V., Shannon, P.M., McGrane, K., Readman, P.W., Jacob, A.W.B., Keary, R., Kenyon, N.H., 2001. Slope instability and sediment redistribution in the Rockall Trough: constraints from GLORIA. In: Shannon, P.M., Haughton, P.D.W., Corcoran, D.V. (Eds.), The Petroleum Exploration of Ireland's Offshore Basins, Special Publication-Geological Society of London, pp. 439–454.

van Aken, H.M., Becker, G., 1996. Hydrography and trough-flow in the north-eastern North Atlantic Ocean: the NANSEN project. Prog. Oceanogr. 38, 297–346.

van Kreveld, S.A., Knappertsbusch, M., Ottens, J., Ganssen, G.M., van Hinte, J.E., 1996. Biogenic carbonate and ice-rafted debris (Heinrich layer) accumulation in deep-sea sediments from a Northeast Atlantic piston core. Mar. Geol. 131, 21–46.

van Ledden, M., van Kesteren, W.G.M., Winterwerp, J.C., 2004. A conceptual framework for the erosion behaviour of sand–mud mixtures. Cont. Shelf Res. 24, 1–11.

van Weering, T.C.E., de Rijk, S., 1991. Sedimentation and climate-induced sediments on Feni Ridge Northeast Atlantic Ocean. Mar. Geol. 101, 49–69.

van Weering, T.C.E., de Stigter, H.C., Balzer, W., Epping, E.H.G., Graf, G., Hall, I.R., Helder, W., Khripounoff, A., Lohse, L., McCave, I.N., Thomsen, L., Vangriesheim, A., 2001. Benthic dynamics and carbon fluxes on the NW European continental margin. Deep-Sea Res. II 48, 3191–3221.

Venz, K.A., Hodell, D.A., Stanton, C., Warnke, D.A., 1999. A 1.0 Myr record of glacial North Atlantic Intermediate Water variability from ODP site 982 in the northwest Atlantic. Paleoceanography 14 (1), 42–52.

Viana, A.R., Faugères, J.-C., Stow, D.A.V., 1998. Bottom-current-controlled sand deposits — a review of modern shallow- to deep-water environments. Sediment. Geol. 115, 53–80.

Wang, Z., Mysak, L.A., McManus, J.F., 2002. Response of the thermohaline circulation to cold climates. Paleoceanography 17, 1–12.

Warren, W.P., 1992. Drumlin orientation and the pattern of glaciation in Ireland. Sver. Geol. Unders. Res. Pap. Ser. Ca 81, 359–366.

Weaver, P.P.E., Wynn, R.B., Kenyon, N.H., Evans, J., 2000. Continental margin sedimentation, with special reference to the north-east Atlantic margin. Sedimentology 47, 239–256.

Wold, C.N., 1994. Cenozoic sediment accumulation on drifts in the northern North Atlantic. Paleoceanography 9, 917–941.